AN ABSTRACT OF THE THESIS OF

Bruce Wilson McClelland (Name) for the Doctor of Philosophy (Degree)

in Chemistry (Major) presented on May 5, 1971 (Date)

Title: ELECTRON-DIFFRACTION INVESTIGATIONS OF THE MOLECULAR STRUCTURES OF SOME OXIDES OF NITROGEN:

I. DINITROGEN TETROXIDE (N_2O_4)

II. DINITROGEN PENTOXIDE (N_2O_5)

Abstract approved: Redacted for Privacy

Kenneth Hedberg

The molecular structure of gaseous N_2O_4 has been reinvestigated at -21°C by the method of electron diffraction. The results confirm the planar D_{2h} symmetry of the molecule, and indicate an even longer N-N bond than found in previous investigations. Despite this extraordinarily long bond (much longer than expected for an N-N single bond), the molecule appears to exhibit only a small amount of torsional motion. The principal distance (r_a) and mean amplitude (ℓ_a) values found in the investigation are: r(N-N) = 1.782 Å (0.0083), r(N-O) = 1.190 Å (0.0018), ∠ONO = 135.39° (0.58), ℓ(N-N) = 0.0816 Å (0.0178), ℓ(N-O) = 0.0381 Å (0.0019), ℓ(O...O) (across the nitro-group oxygens) = 0.0493 Å (0.0040), ℓ(O...O) (on the same side of the molecule through two nitrogen atoms) = 0.0970 Å (0.0167), ℓ(O...O)

(across the molecule through two nitrogen atoms) = 0.0730 Å (0.0114). The parenthesized quantities are 2σ, and include estimates of systematic error.

The molecular structure of gaseous N_2O_5 has been reinvestigated at -11°C by the method of electron diffraction. The results confirm the $O_2N\text{-}O\text{-}NO_2$ configuration and are consistent with C_{2v} symmetry for the $O\text{-}NO_2$ groups. The principal distance (r_a) and mean amplitude (ℓ_a) values, as determined by a least squares procedure, are: r(N-O) = 1.499 Å (0.0060), r(N=O) = 1.188 Å (0.0015), $\angle$ O=N=O = 133.31° (0.82), $\angle$ NON = 112-116°, ℓ(N-O) = 0.0669 Å (0.0064), ℓ(N=O) = 0.0349 Å (0.0018), ℓ(O...O) (between the nitro group oxygens) = 0.0421 Å (0.0045), ℓ(O...O) (between the central oxygen and the nitro group oxygens) = 0.0710 Å (0.0076). (The parenthesized quantities are 2σ, and include estimates of systematic error.) The range of values given for the NON angle reflects the difficulty of determining the N...N distance in the presence of other nearly similar distances, including some of those sensitive to torsional motion. The potential involving torsional motion is undoubtedly complicated, but the structural results can be explained in terms of strong steric repulsions between oxygens of different nitro groups superimposed on a moderate, restricted rotation of the groups.

Electron-Diffraction Investigations of the Molecular Structures of Some Oxides of Nitrogen: I. Dinitrogen Tetroxide (N_2O_4) II. Dinitrogen Pentoxide (N_2O_5)

by

Bruce Wilson McClelland

A THESIS

submitted to

Oregon State University

in partial fulfillment of
the requirements for the
degree of

Doctor of Philosophy

June 1971

APPROVED:

Redacted for Privacy

Professor of Chemistry
in charge of major

Redacted for Privacy

Chairman of Department of Chemistry

Redacted for Privacy

Dean of Graduate School

Date thesis is presented May 5, 1971

Typed by Cheryl E. Curb for Bruce Wilson McClelland

ACKNOWLEDGEMENTS

I am especially grateful to Professor Kenneth Hedberg for taking me on as his graduate student.

I would like to thank cand. real Grete Gundersen for her guidance during the N_2O_4 investigation, and Professor Hedberg for his guidance during the N_2O_5 investigation. I would also like to thank cand. real Lise Hedberg for her helpful discussions concerning the N_2O_5 investigation.

I would like, too, to thank fellow graduate students Michael M. Gilbert and John Neisess for their many helpful discussions.

Finally, I would like to thank my wife, Donia Carolyn, for her patience and help during the time this work was being done.

TABLE OF CONTENTS

LIST OF TABLES

LIST OF TABLES (Cont.)

LIST OF FIGURES

ELECTRON-DIFFRACTION INVESTIGATIONS OF THE MOLECULAR STRUCTURES OF SOME OXIDES OF NITROGEN: I. DINITROGEN TETROXIDE (N_2O_4) II. DINITROGEN PENTOXIDE (N_2O_5)

GENERAL INTRODUCTION

The oxides of nitrogen have been of considerable interest to chemists for many years; the recent concern with air pollution has deepened that interest. Dinitrogen tetroxide (N_2O_4) and dinitrogen pentoxide (N_2O_5) are the most complex of the nitrogen oxides, and their chemistry has been the subject of many studies since the beginning of this century. Yet it is only within the last 15 years that a relatively complete description of the molecular structure of covalent N_2O_4 has been established; and a reliable description of the shape of covalent N_2O_5 has been heretofore unknown.

The molecular structures of both N_2O_4 and N_2O_5 may be studied by the method of gaseous electron diffraction. The former is the dimer of the free radical nitrogen dioxide (NO_2), and the well-known equilibrium between them,

$$N_2O_4 \rightleftharpoons 2NO_2,$$

is strongly temperature dependent: $K_{eq} = 1.78 \cdot 10^{-3}$ atm at -23.2°C; $K_{eq} = 5.18 \cdot 10^{1}$ atm at 126.8°C (Hisatsune, 1961). The high vapor pressure of the solid (m.p. -11.2°C [Weast, 1967]) at low temperatures (where K_{eq} is small), e.g., 40 mm at -23.9°C, makes the

collection of gaseous electron diffraction data for N_2O_4 straightforward. N_2O_5, on the other hand, is thermally unstable, the vapor having a half-life of about ten days at 0°C, and of less than eight hours at 25°C (Schott and Davidson, 1958). Again, however, the high vapor pressure of the solid (m.p. 30°C [Weast]) at low temperatures, e.g., 10 mm at -16.7°C, makes the collection of electron diffraction data for N_2O_5 relatively easy.

Since both the theory of gaseous electron diffraction and its use in determining molecular structures have been adequately described elsewhere, for example by Brockway (1936), Glauber and Schomaker (1953), and Waser and Schomaker (1953), and repeatedly summarized in theses from this department (Barnhart, 1964; Blank, 1964; Crawford, 1959; Ryan, 1965), only a brief summary of the method will be given here.

When a stream of the vapor of the compound under investigation is injected from a nozzle into a highly collimated beam of monochromatic electrons, the interaction of the electrons with the potential field of the molecules produces a symmetric distribution of scattered electrons in the form of cones coaxial with the undiffracted beam. This diffraction pattern is recorded on a photographic plate mounted perpendicular to the undiffracted beam. Since the intensity of the scattered electrons decreases rapidly with the scattering angle, a spiral-shaped "rotating sector" is employed to mechanically reduce

the intensity at small angles relative to that at larger angles. It is mounted parallel to and just above the photographic plate, with its rotation axis coincident with the undiffracted beam. The intensity I_p recorded on the photographic plate is related to the total scattered intensity I_t by $I_p = I_t \alpha(r) \cdot \cos^3 2\theta$, where $\alpha(r)$ is the sector correction, and 2θ is the scattering angle. The geometric factor $\cos^3 2\theta$ takes into account the fact that a flat photographic plate is not everywhere equidistant from the scattering point. The total intensity I_t is composed of essentially four parts, of which only one, I_m/s^4 (where s is defined below), depends on the molecular structure. The other three terms may be conveniently regarded as a background, B_t/s^4, so that

$$I_t = \frac{I_m}{s^4} + \frac{B_t}{s^4} \quad .$$

To obtain the structure sensitive part of the intensity, then, the density of exposed photographic plates is measured on a microdensitometer to obtain I_p as a function of s, and converted to $s^4 I_t$ according to

$$s^4 I_t = \frac{s^4 I_p}{\alpha(r) \cos^3 2\theta} \quad .$$

The background B_t is subtracted from $s^4 I_t$ to obtain I_m, which is then multiplied by s to give sI_m, defined by

$$sI_m = k \sum_{i,j} \frac{A_i A_j}{r_{ij}} \cdot e^{-\ell_{ij}^2 s^2/2} \cdot \cos |\eta_i - \eta_j| \cdot \sin r_{ij} s \quad , \qquad (1)$$

where the symbols have the following meaning:

$s = \frac{4\pi}{\lambda} \sin\theta$, where 2θ is the scattering angle, and λ is the electron wavelength

k = scale constant

r_{ij} = internuclear distance between atoms i and j

A_i = electron scattering factors multiplied by s^2

ℓ_{ij} = root-mean-square amplitudes of vibration associated with r_{ij}

η_i = phase shift factor

The problem of determining the molecular structure becomes one of analyzing the curve sI_m to obtain values of r_{ij} and ℓ_{ij}. If sI_m is multiplied by $Z_i Z_j / A_i A_j$, where Z_i is the atomic number of atom i, to give $I'_m(s)$ having essentially constant coefficients, then the radial distribution curve $D(r)$, which gives the distribution of distances in the molecule, may be obtained by calculating the Fourier transform of $I'_m(s)$:

$$D(r) = \frac{2}{\pi} \int_0^\infty I'_m(s) \sin rs \, ds.$$

Since the curve $I'_m(s)$ is not continuous and is of finite length, $D(r)$ in practice is calculated according to

$$D(r) = \frac{2}{\pi} \Delta s \sum_{s_{min}}^{s_{max}} I'_m(s) e^{-Bs^2} \sin rs, \qquad (2)$$

where the damping factor B is usually estimated from $e^{-Bs^2} = 0.1$

at $s = s_{max}$. D(r) consists of a sum of peaks, each one a Gaussian (in the harmonic oscillator approximation used above), whose position represents an internuclear distance r_{ij}, whose area is proportional to nZ_iZ_j/r_{ij}, where n is the multiplicity of distance r_{ij}, and whose half-width at half-height $\Delta r_{\frac{1}{2}}$ is related to the root-mean-square vibrational amplitude ℓ_{ij} by

$$\frac{1}{2} = \exp\left[\frac{-\Delta r_{\frac{1}{2}}^2}{2\ell_{ij} + 4B}\right].$$

From the radial distribution curve, a trial structure of the molecule can often be deduced. Final values of the structural parameters are usually obtained by least squares refinement of the trial structure, which will be discussed more fully later.

PART I. DINITROGEN TETROXIDE (N_2O_4)

Introduction

The structure of N_2O_4 has been the subject of a considerable number of experimental investigations. The first complete structure determination came from the single crystal x-ray study by Broadley and Robertson (1949) of the stable cubic crystalline material. They found the N_2O_4 molecule to have planar (D_{2h}) symmetry in the solid state, and reported the following geometrical parameters: N-N bond, 1.64 ± 0.03 Å; N-O bond, 1.17 ± 0.03 Å; $\angle$ ONO, $126^\circ \pm 1^\circ$. The value for the N-N bond length may be compared with the values 1.45 Å in N_2H_4 (hydrazine) (Morino, Iijima, and Muratu, 1960), and 1.49 Å in N_2F_4 (tetrafluorohydrazine) (Cardillo and Bauer, 1969; Gilbert, 1971). Later, Wiener and Nixon (1957) carried out infrared studies on crystalline N_2O_4, and found their spectra to be consistent with the results of Broadley and Robertson. In 1956, the results of a gaseous electron-diffraction study of N_2O_4 were published (Smith and Hedberg, 1956). Smith and Hedberg concluded that N_2O_4 was also planar in the vapor state, but found values for the geometrical parameters that were different from those reported by Broadley and Robertson; these values are shown in Table 11. At about the same time, Snyder and Hisatsune (1957) concluded from infrared studies on solid, liquid, and gaseous N_2O_4, that the molecule was planar in all three phases. In addition,

they estimated the barrier to internal rotation in the molecule to be 2.9 kcal/mole. In 1959, Fateley, Bent, and Crawford, Jr. (1959) reported that their matrix isolation studies of N_2O_4 at liquid-helium temperatures had yielded infrared spectroscopic evidence for two unstable forms of N_2O_4, which they identified as a staggered (D_{2d}) form and an unsymmetrical ONO-NO_2 form. In the next year, results of similar studies carried out at liquid-nitrogen temperatures were published (Hisatsune, Devlin, and Wada, 1960) which confirmed the existence of the two unstable N_2O_4 species. In the same year, Hisatsune, Devlin, and Califano (1960) reported the calculation of Urey-Bradley potential constants for N_2O_4. They obtained a reasonable set of constants using the electron-diffraction values of Smith and Hedberg for the molecular parameters. Then, in 1963, an x-ray diffraction study of the structure of an unstable monoclinic form of crystalline N_2O_4 was reported by Groth (1963). His results (N-N bond, 1.75 Å, N-O bond, 1.21 Å, and $\angle$ ONO, 135°) were in satisfactory agreement with those of Smith and Hedberg. Finally, Cartwright and Robertson (1966) reinvestigated the cubic crystalline form of N_2O_4, this time as a function of temperature, and found, at -13°C, an N-N bond length of 1.745 $\pm$0.014 Å, an N-O bond length of 1.214 $\pm$0.010 Å, and an ONO angle of 133.7° $\pm$1.2°, in good agreement with the results of Smith and Hedberg and of Groth.

While the structure of N_2O_4 was apparently well established, it was felt that a new electron-diffraction investigation of the molecule would be worthwhile for several reasons. First, previous investigations of the gaseous compound did not entirely rule out the possibility of the presence of a small amount of a non-planar form at normal temperatures, and it was thought that a new investigation might yield some additional information about this aspect of the structure. Second, at the time that the earlier electron-diffraction study of Smith and Hedberg was carried out, there was some uncertainty about the electron wavelength in the Oslo electron-diffraction apparatus used in collecting their data, which produced a corresponding uncertainty in the overall size of the molecule. Experiments have shown that the electron wavelength in the Oregon State apparatus is accurately known (Plato, Hartford, and Hedberg, 1970), so that the molecular-size problem could be virtually eliminated by a new investigation. Finally, improved methods of analyzing electron-diffraction data have been introduced since the work of Smith and Hedberg was undertaken, such as the mechanical spinning of the electron-diffraction plates while measuring photographic density (as opposed to the oscillation of the plates), and the use of least-squares refinement procedures to determine the best values for the molecular parameters. These improvements allow a more precise determination of the molecular-structure parameters.

Experimental and Data Reduction

A mixture of NO_2 and N_2O_4 was prepared by condensing NO_2 gas in a bulb equipped with a stopcock and T joint which could be affixed directly to the electron-diffraction apparatus. Commercial-grade NO_2 (Matheson) was used without further purification. Electron-diffraction photographs were made with the Oregon State apparatus by Mr. William Hartford, using a rotating sector with angular opening proportional to r^3, on 5 in. x 7 in. and 8 in. x 10 in. Kodak process plates. Initially, it had been planned to study the NO_2-N_2O_4 system equilibrium using electron-diffraction data, and so a large number of photographs were prepared, at several different nozzle temperatures. For the present study, however, only the best plates at the lowest temperatures were used, so as to maximize the amount of N_2O_4 present in the NO_2-N_2O_4 mixtures. Table 1 summarizes the experimental data for these plates. To be particularly noted in Table 1 is that the plates at the middle nozzle-to-plate distance were exposed with an electron accelerating voltage of 47.3 kV, while the long and short distance plates were exposed with a 44.0 kV beam. This will be further discussed later.

Initially, ten plates prepared with a nozzle temperature of about -21°C were found to be of sufficiently good quality to analyze. Each of these plates was scanned on a modified Joyce-Loebl microdensitometer while being rotated about the axis of the diffraction rings

(Gundersen and Hedberg, 1969). The resulting density data were reduced in the manner previously described (Gundersen and Hedberg; Hedberg and Iwasaki, 1962), and the results plotted. Because of relatively low signal-to-noise ratios, the data from two of the plates were discarded.

Preliminary smoothed backgrounds were drawn through each of the results of the data-reduction procedure, and the differences between these results and the backgrounds were calculated and multiplied by s to give preliminary experimental values of sI_m, as defined by (1). The data-reduction results, multiplied by appropriate factors that put the curve-background differences sI_m on the same scale, together with the final backgrounds, are shown in Figure 1. These final backgrounds include small corrections to the preliminary backgrounds, corrections which were suggested as the structure refinement proceeded. The final curves sI_m, resulting from the subtraction of the final backgrounds from the data-reduction results, are shown in Figure 2 and listed in Tables 2-9.

It should be noted here that when the data reduction of the N_2O_4 plates took place, no blackness correction (which takes into account the non-linear response of photographic emulsions to exposing intensity) was available for Oregon State plates. After this study of N_2O_4 was completed, and the figures for the thesis were made, it was discovered that portions of the middle camera plates were unacceptably

dense. A final refinement was therefore carried out using only acceptable data. The resulting parameter values differed very little from those previously found, so that the intensity and radial distribution curves were indetectably different, making it unnecessary to redraw the figures.

Preliminary Structure Analysis

In order to calculate an experimental radial distribution curve, a composite curve was made by scaling and averaging the preliminary curves sI_m in their overlap regions. Figure 3 shows the experimental composite curve similarly calculated from the final curves sI_m. The composite curve was then converted to the constant coefficient curve I'_m (s) by multiplying each point by $(Z_N Z_O / A_N A_O)$ where Z_N and Z_O are the atomic numbers of nitrogen and oxygen, respectively. A preliminary experimental radial distribution curve D(r) was then calculated according to (2) using B = 0.001, following which a theoretical intensity curve was calculated according to (1) using the distance and amplitude values suggested by the preliminary D(r) curve. These results were used to make small background corrections in the observed intensity curves and to supply the missing intensity data in the range $0 \leq s \leq 0.75$. The radial distribution curve was then recalculated using data over the range $0 \leq s \leq 47.75$, with experimental data for the range $3.25 \leq s \leq 47.75$. When the structure refinement was

completed and the final model for N_2O_4 determined, a final radial distribution curve was calculated from the experimental curve of Figure 3 using theoretical data corresponding to that final model in the region $0 \leq s \leq 3.0$; this final experimental D(r) curve is shown in Figure 4.

A planar D_{2h} model for N_2O_4 (shown in Figure 5) was readily seen to fit the peaks of the experimental radial distribution curve as follows: 1.19 Å, N-O bonds; 1.77 Å, N-N bond; 2.20 Å, $O_1 \ldots O_2$; 2.5 Å, N...O; 2.7 Å, $O_1 \ldots O_1'$; 3.47 Å, $O_1 \ldots O_2'$. Several details were not obvious, however. Thus, the amount of NO_2 present with N_2O_4 when the plates were exposed could not immediately be ascertained, since the corresponding N-O and O...O distances in the two compounds are almost identical. Also, while a planar model appeared to fit the radial distribution curve well, it was not obvious that a model involving a small deviation from planarity might not provide an even better fit. Least squares refinement procedures were therefore introduced in order to elucidate these aspects of the structure, and to give the best values for the N_2O_4 parameters.

Structure Refinement

Refinement of the structure was carried out by the method of least squares based upon intensity curves (Hedberg and Iwasaki, 1964), using the individual curves sI_m. Such a refinement consists of

obtaining the best fit, within the least-squares criteria, of a theoretical intensity curve to each of the observed curves of Figure 2 simultaneously. The theoretical curves are calculated according to equation (1), where the modified scattering factors A_i and the phase factors η_i are functions of both the accelerating voltage and s. The computer program that carries out the least-squares refinement (Hedberg, Ryan, and Hedberg, 1968) can use a set of factors A_i and η_i for one accelerating voltage only in operating with the curves sI_m. Before refinement began, then, it was necessary to determine if the relatively large difference between the accelerating voltage (47.3 kV) used for the middle distance plates and the voltage (44.0 kV) used for the long and short distance plates might make the respective sets of data incompatible for such a refinement procedure. Evidently, if $(A_{44.0}/A_{47.3})_N = (A_{44.0}/A_{47.3})_O = k$, a constant for all s, and if $(\eta_N-\eta_O)_{44.0} = (\eta_N-\eta_O)_{47.3}$ for all s, there would be no effect whatever in refining the two sets of data simultaneously. Modified scattering factors A_i and phase factors η_i for oxygen and nitrogen at both 47.3 kV and 44.0 kV were obtained from Cox and Bonham's table (Cox and Bonham, 1967) in the manner previously described (Gundersen and Hedberg), and compared as indicated. It was found that $(A_{44.0}/A_{47.3})_N = (A_{44.0}/A_{47.3})_O = k$, but that $(\eta_N-\eta_O)_{44.0} \neq (\eta_N-\eta_O)_{47.3}$. However, since η_N and η_O are nearly equal, the difference between $(\eta_N-\eta_O)_{44.0}$ and $(\eta_N-\eta_O)_{47.3}$ was considered to be sufficiently small to be

neglected over the s range that the data covered. Simultaneous refinement of the data from all three nozzle-to-plate distances was thus carried out using scattering factors A_i and phases η_i for an accelerating voltage of 44.0 kV.

The refinement was carried out using a unitary weight matrix. The parameters refined were the N-N bond length, the N-O bond length, the ONO angle, all six N_2O_4 vibrational parameters, the mole fraction of N_2O_4, and the mole fraction of NO_2. The molecular parameters for NO_2 were fixed at values found in a previous investigation (Blank), and are listed in Table 10. Initially, the twist angle between the NO_2 groups was fixed at 0^o. At a late stage in the refinement this angle was introduced as an additional parameter. The angle refined to a value of about $5^o \pm 10^o$, and was felt to reflect torsional vibrations about the N-N bond, rather than to represent a real deviation from planarity. (The effects of such vibrations can be seen in the slight asymmetry of the $O_1 \ldots O_2'$, peak at 3.47 Å in the radial distribution curve.) For the remainder of the refinement, then, the twist angle was again held fixed at 0^o.

The refinement proceeded smoothly, and converged to acceptable values for all parameters. Table 11 gives what is considered the best parameter values for N_2O_4, and their associated error estimates. These are based on the final refinement carried out using all the long and short distance data and the middle distance data in the interval

$12.0 \leq s \leq 32.25$ only. The error estimates were calculated from the formulas

$$2\sigma_r = 2[2\sigma_{LS}^2 + (0.0005r)^2]^{1/2},$$
$$2\sigma_\ell = 2[2\sigma_{LS}^2 + (0.02\ell)^2]^{1/2}, \qquad (3)$$
$$2\sigma_L = 2\sqrt{2}\,\sigma_{LS},$$

where the quantities σ_{LS}^2 are obtained directly from the least squares analysis. The coefficient 2 associated with σ_{LS}^2 reflects possible correlation among the observations, the factor 0.0005 takes into account errors in electron wavelength, camera distance, and sector calibration, and the factor 0.02 reflects error in converting photographic density to scattered intensity. Theoretical intensity and radial distribution curves corresponding to the parameters from the refinement of all the data, and the differences between these and the corresponding experimental curves, are shown in Figures 3 and 4. The correlation matrix for the final refinement resulting in the values of Table 11 is given in Table 12.

Because of the significant amount of NO_2 apparently present in the N_2O_4-NO_2 sample mixture during the data collection, several additional refinements were attempted. First, attempts were made to refine the NO_2 parameters simultaneously with those of N_2O_4. However, all such attempts either failed to converge, or failed to converge to reasonable values for the NO_2 parameters. During such refinement attempts, however, the N_2O_4 parameters changed little.

Second, because the NO_2 parameters held fixed during the N_2O_4 refinement were for NO_2 at 107°C, whereas the N_2O_4-NO_2 data being refined was for sample at -21°C, it was desirable to use NO_2 vibrational amplitudes for a temperature nearer -21°C and refine the N_2O_4 parameters as before, i.e., with all NO_2 parameters held fixed. Theoretical values for the vibrational amplitudes of NO_2 at 107°C and 0°C were supplied by Sven J. Cyvin of the Institute of Physical Chemistry, Technical University of Norway, Trondheim, and are given in Table 10. The differences between the corresponding amplitudes at the two temperatures were subtracted from the experimental values at 107°C to give "corrected" experimental amplitudes: these are also given in Table 10. These "corrected" experimental NO_2 amplitudes were then used in a refinement of the N_2O_4 parameters based on the composite intensity curve of Figure 3, all NO_2 parameters being held fixed as before, and the results were compared with a similar refinement using the experimental 107°C amplitudes for NO_2. The comparison showed that the change in the NO_2 amplitudes made essentially no difference in the values obtained for the N_2O_4 parameters: no attempt was made, therefore, to redo the simultaneous refinement of the individual sI_m curves using the "corrected" NO_2 vibrational amplitudes.

Discussion

The results of the previous electron-diffraction work of Smith and Hedberg are shown in Table 11. The present work essentially confirms those results so far as the molecular shape is concerned. However, a close comparison of the two sets of results indicates some discrepancies in the values of some of the parameters. It is evident that a scale-factor error in one of the investigations could account for a large part of those discrepancies involving the geometrical parameters: the Smith and Hedberg model for N_2O_4 is smaller than the model obtained from the present study. It is felt that this scale-factor error is most likely to be found in the work of Smith and Hedberg and could have resulted from an error in the electron wavelength: as indicated earlier, there was some uncertainty in the electron wavelength in the Oslo apparatus when the earlier N_2O_4 data were collected. Beyond this, the remaining differences between the two results may be due to a more complete refinement of the data in the present study than was carried out in the earlier work.

The present work confirms all the previous work on N_2O_4 supporting the planar model for the molecule in the gas phase: the experimental radial distribution curve (Figure 4) gives no indication of internal rotation or of observable amounts of N_2O_4 with symmetry D_{2d}; and both the experimental radial distribution curve and the least-

squares refinement indicate that other deviations from planarity are small or nonexistent.

Two features of the structure of N_2O_4 are notable. First, the geometry of the NO_2 groups in N_2O_4 is very similar to the geometry found for NO_2 (Bird, 1956; Blank). Thus, when the NO_2 radical dimerizes, its geometry changes only a little. Second, the root-mean-square amplitude associated with the N-N bond is very large. The value of 0.0816 Å found in this study may be compared to the N-N amplitude found in N_2F_4 of about 0.046 Å (Cardillo and Bauer; Gilbert). This large amplitude is not surprising in view of the relative ease with which N_2O_4 dissociates into NO_2 radicals.

Two other aspects of the structure of N_2O_4 are quite remarkable; first, the very long (and weak) N-N bond; and second, the greater stability of the planar form relative to a twisted form. There have been many attempts to explain these features in terms of the bonding in the molecule. Smith and Hedberg proposed that the N-N bond is largely of π rather than σ character. The requirement of the overlap of the orbitals involved in a π bond would account for the planarity of the molecule, and the poor overlap qualities of such orbitals in the bond direction would account for the length of the bond. Such a proposal has been rejected, however (Brown and Harcourt, 1965; Pauling, 1960). Pauling explains the long N-N bond in terms of the stability of the three electron bond in each of the two NO_2 molecules that compose

the dimer. This stability tends to keep the odd electrons in the two NO_2 molecules from settling down on the nitrogen atoms so that the required N-N bond can be formed. The observed planarity of the molecule is explained by Pauling in terms of a small amount of π interaction. Other proposals to explain these features of the structure of N_2O_4 are somewhat complex, but most theoretical studies indicate that nitrogen-nitrogen π bonding accounts for the planarity of N_2O_4. See Harcourt (1966), and Redmond and Wayland (1968), and the references cited therein, for a review of these studies.

PART II. DINITROGEN PENTOXIDE (N_2O_5)

Introduction

In contrast to N_2O_4, a complete picture of the geometry of N_2O_5 has not been established. However, considerable information about the structure of the molecule has been deduced from many different types of experiments, and is summarized below. A model of N_2O_5 is shown in Figure 6 to help clarify this discussion of the previous results. For the sake of convenience, the symbols N-O and N=O will be adopted to refer to the bonds corresponding to N_1-O_5 and N_1-O_1, respectively. While the bond corresponding to N_1-O_5 is a single bond, the bond corresponding to N_1-O_1 is not a true double bond (Pauling), and the symbolism N=O is not meant to imply that it is.

N_2O_5 vapor consists of covalent N_2O_5 molecules. However, it has been shown that this vapor dissociates into $NO_2 + NO_3$ (Schott and Davidson, and references cited therein). In highly polar solvents, N_2O_5 ionizes into $NO_2^+ + NO_3^-$ (Chedin, 1935). Also, an x-ray crystallographic study (Grison, Eriks, and de Vries, 1950) and an infrared study (Teranishi and Decius, 1954) have shown that in the crystalline state, N_2O_5 exists as the ionic compound nitronium nitrate ($NO_2^+NO_3^-$). Rapid sublimination of the compound onto a cooled (-180°C) window of a low temperature infrared cell, however, produces a solid containing covalent molecules (Teranishi and Decius; Hisatsune, Devlin, and

Wada, 1962). On the basis of their infrared spectra of covalent N_2O_5 in both the vapor and unstable solid states, and taking into account the earlier work, Hisatsune, Devlin, and Wada (1962) concluded that the configuration of the covalent molecule is $O_2N\text{-}O\text{-}NO_2$, with C_2 axis of the nitro groups coinciding with the central N-O bonds. Taking into account the dipole moment of N_2O_5 (Lewis and Smyth, 1939), Hisatsune, Devlin, and Wada (1962) also concluded that the central N-O-N group was bent and of symmetry C_{2v}. However, they were unable to determine the relative orientation of the two $-NO_2$ (nitro) groups or the value of the central valence angle NON, though a Urey-Bradley force field calculation based on a planar molecule and a central angle of 150° gave a reasonable correspondence of calculated and observed infrared absorption frequencies.

Two electron-diffraction studies of N_2O_5 have been carried out. Akishin, et al. (1962) reported N_2O_5 to be bent, with non-planar C_{2v} symmetry. Geometrical parameters were also reported, and are given in Table 26. Mean amplitudes of vibration were not given in the report by Akishin, et al., however. Also included in Table 26 are the preliminary results of an electron-diffraction study carried out by Hedberg and Hedberg (1965), which was never carried to completion. A comparison of the results of Akishin, et al., and Hedberg and Hedberg indicate considerable disagreement in regards to the values of the geometrical parameters of the molecule. Further,

Hedberg and Hedberg could not determine the long range structure of the N_2O_5 molecule, due to the "washed-out" character of their experimental radial distribution curve in the region $r > 2.5$ Å; however, their data did not allow the non-planar C_{2v} symmetry reported for the molecule by Akishin, et al. Hedberg and Hedberg also expressed some uncertainty in the assumption of C_{2v} symmetry for the central NON group because of the large amplitude of vibration that they found associated with the N-O bond; it was felt that the large amplitude could either be real, or else reflect the presence of two unresolved N-O peaks.

Because of the inconclusiveness of the results of Hedberg and Hedberg, and because of the conflicts of those results with those of Akishin, et al., it was felt worthwhile to reopen the investigation of the molecular structure of N_2O_5, using new electron-diffraction data. Relative peak areas in the experimental radial distribution curve of Hedberg and Hedberg suggested that some NO_2 (which is one of the decomposition products of N_2O_5), and therefore some N_2O_4, were present when the data were collected. The presence of such impurities would tend to obscure the long range structural information about N_2O_5 in their radial distribution curve, as well as affect the apparent values of the geometrical parameters of the molecule. It was hoped, then, that new data obtained using pure N_2O_5 might give more conclusive results concerning the structure of the molecule.

Experimental and Data Reduction

N_2O_5 was prepared by the ozonolysis of NO_2, according to the equation

$$2NO_2 + O_3 \longrightarrow N_2O_5 + O_2.$$

The procedures and apparatus used were those given by Tyree (1967), with modifications as follows. First, because of the unavailability of a commercial ozonizer, a small ozonizer tube after the design of Jolly (1960) was constructed, and energized by a 12 kV neon sign transformer. Second, oxygen used to generate the ozone was first passed through a glass U-tube packed with glass wool and immersed in a dry ice-methanol slush, then through a P_2O_5 drying column, before being introduced into the ozonizer (Schott and Davidson). Third, the NO_2-O_3 mixture was cooled to 0^oC before being mixed in the mixing condensor containing glass helices. Because of the small ozone source, the overall size of the preparative apparatus was substantially smaller than that of Tyree.

Commercial (National Cylinder Gas) O_2 and commercial (Matheson) NO_2 were used in all preparative runs. A typical preparative run of three hours produced about one gram of N_2O_5. Each N_2O_5 sample prepared was checked for the presence of NO_2 by warming the N_2O_5 to 0^oC in an evacuated vessel one inch in diameter by eight inches long and observing the presence or absence of the characteristic brown color of NO_2 in the vapor above the N_2O_5 while looking

through the length of the vessel (Schott and Davidson, 1958). Once prepared and checked for purity, the N_2O_5 samples were stored under vacuum in liquid nitrogen until used.

Twenty-two electron-diffraction photographs of N_2O_5 were prepared, and of these, nine were analyzed in the same manner as described for the N_2O_4 plates. The data from eight of these plates were subsequently used in the structure determination. The experimental data for these eight plates are given in Table 13.

As in the case of N_2O_4, no blackness correction was available when the data from the N_2O_5 plates were initially analyzed. Considerable work was done using the data uncorrected for blackness. When the blackness correction became available (Neisess, 1971), it was applied to three long-distance plates which were found to be unacceptably dense. The earlier work was corrected in those cases where it was felt that omission of the blackness correction might contribute to erroneous results. All figures, tables, results, and conclusions are based on blackness-corrected data.

Preliminary Structure Analysis

The results of the data-reduction procedure for N_2O_5 were used to calculate a preliminary radial distribution curve D(r) in the manner described for N_2O_4 using B = 0.0007. This experimental curve D(r) did not immediately suggest a suitable model for N_2O_5 from which

background changes, the necessity for which was clearly apparent, could be calculated. It was therefore necessary to obtain these changes without reference to a theoretical intensity curve by using the criterion that $D(r) \geq 0$ for all $r \geq 0$ (Hauptman and Karle, 1950), which is approximately valid in the event that the various atoms in the structure under study have nearly equal atomic numbers. Using theoretical data in the interval $0 \geq s \geq 0.75$ from a theoretical curve corresponding to a model suggested by the preliminary curve D(r) that provided a good fit to that curve at r values less than 2.5 Å, but only an approximate fit at r values greater than 2.5 Å, backgrounds were adjusted until $D(r) \geq 0$ was properly satisfied. The final curves sI_m, resulting from the subtraction of the final backgrounds from the data-reduction results, are shown in Figure 7 and listed in Tables 14-21; and the final composite curve, calculated from the final curves sI_m, is also shown in Figure 7. The final experimental radial distribution curve, which was calculated from the final composite curve, is shown in Figure 8. (In calculating the experimental curve D(r) of Figure 8, data in the interval $0 \geq s \geq 2.75$ were obtained from the theoretical intensity curve corresponding to a free-rotation model for N_2O_5, to be described later.)

A preliminary analysis of the radial distribution curve confirmed some of what had been previously established about the N_2O_5 molecule. The distances from the first three peaks suggested the

configuration $O_2N\text{-}O\text{-}NO_2$, as follows: 1.19 Å, N=O double bonds; 1.50 Å, N-O single bonds; 2.2 Å, the two different O. . . O distances in an $O\text{-}NO_2$ group corresponding to an O=N=O angle of about 135°. The relative areas (and therefore the distance multiplicities) of the first three peaks were in agreement with the indicated configuration: experimental areas found were 4.24:2:6.56 for the 1.19 Å, 1.50 Å, and 2.2 Å peaks, respectively, corresponding well to the theoretical values 4:2:6.86. No other chemically logical arrangement of five oxygen and two nitrogen atoms gives such a set of single and double bond multiplication. Support for the idea that the molecule has a symmetrical N-O-N grouping was provided by the half-width at half-height of the peak at 1.50 Å, which indicated a larger than normal, but nonetheless reasonable amplitude for the N-O bond.

Further analysis of the experimental radial distribution curve D(r) indicated that the central valence angle NON had a value in the range 105°-130°. The lower limit was indicated by the relative areas of the first three peaks: an angle smaller than 105° associates the N. . . N distance with the 2.2 Å peak and gives to it too great a weight relative to the other peaks. With an O=N=O angle of about 135° (clearly indicated by the positions and shapes of the first three peaks), it was found that no orientation of the nitro groups would give distances less than about 2.6 Å if the central NON angle was greater than 130°; since the experimental D(r) curve was positive at 2.5 Å, and the

corresponding area had to be assigned to rotation-sensitive distances, an upper limit value of 130° for ∠ NON appeared very likely. The relative orientation of the NO_2 groups was not immediately obvious, however, due to the "washed-out" character of the experimental D(r) curve in the region r > 2.5 Å.

In an attempt to determine the relative orientation of the nitro groups, inter-nitro group distance distributions were calculated and plotted for models of N_2O_5 corresponding to every unique relative orientation of the nitro groups obtained by incrementing the nitro group twist angles about the N-O single bonds in amounts of 15°, for various values of the central NON angle. For these calculations, the geometry of the NO_2 group was that obtained from the preliminary analysis of the first three peaks of the experimental radial distribution curve D(r). The results indicated that only certain combinations of relative orientation and NON angle provided approximate fits to D(r) at r values greater than 2.5 Å. Least-squares refinements were carried out using these combinations and the preliminary amplitudes and distances obtained from the first three peaks of the experimental curve D(r) as starting values. Details of the refinement results are not important; they may be simply summarized by saying they suggested rough combinations of nitro-group orientation and an associated NON angle, none of which fit the experimental D(r) curve well at r values greater than 2.5 Å. From careful study of the results it was concluded that no

single orientation of the nitro groups could completely account for the experimental D(r) curve in the region r > 2.5 Å. However, it was found that the values of the distances and amplitudes associated with the O-NO_2 groups obtained from the least-squares analyses were always the same to within very small limits, independent of the orientation of the NO_2 groups. Furthermore, these values provided a very good fit to the experimental curve D(r) for r values less than 2.5 Å. The parameter values for the O-NO_2 groups are shown in Table 22; these values were used in all further calculations carried out in attempts to elucidate the rotation-sensitive structure of the molecule. Final values for these parameters (differing only slightly from those in Table 22) will be given later.

Structure Refinement

The detailed structure analysis of N_2O_5 involved two steps. The first was concerned with the determination of the central NON angle and the elucidation of the conformation of the molecule. The second was concerned with obtaining the best values for the O-NO_2 group parameters.

Since the preliminary work had indicated that no single orientation of the nitro groups could entirely account for the longer-distance details of the experimental radial distribution curve, it became necessary to consider models involving internal motions of these groups.

Procedures for the calculation of theoretical intensity and radial distribution curves for molecules in which torsional motion is important are standard, and were applied to N_2O_5 as follows. Each nitro group was regarded as rotating about its C_2 axis so that the two oxygen atoms moved on a circle of rotation. To calculate an exact theoretical radial distribution curve requires that a suitable average be taken over the infinite number of conformations reflecting all possible orientations of the two NO_2 groups. Such an average, it was found, could be satisfactorily approximated by designating on each of the two circles of rotation 24 positions corresponding to torsional angles of 0^o, 15^o, 30^o, etc. (where 0^o corresponds to a nitro group being coplanar with the central NON group, and the direction of positive angle increase is defined as clockwise rotation), and assigning to each position a weight derived from an assumed hindering potential. The number of conformations in this approximation are thus $24^2 = 576$, of which (because the NO_2 groups were assumed to have a C_2 axis colinear with an N-O bond) only 43 are unique. Of these, conformations having C_2 or C_s symmetry occur eight times, C_{2v} symmetry four times, and all others 16 times. Calculations of theoretical radial distribution curves for models having torsional motion thus required the calculation of individual theoretical radial distribution curves corresponding to the 43 unique conformations using the parameter values in Table 22 with an assumed value of $\angle$NON, multiplication of each of

these curves by the appropriate frequency of occurrence and weight, summation of the weighted curves, and finally, multiplication by an overall scale factor. Results of this calculation were immediately encouraging. For example, crude models with a zero torsional barrier (free rotation) gave generally better fits to the experimental radial distribution curve in the region $r > 2.5$ Å than any of the static models. Figure 9 shows the curve (designated FR) for such a model having an NON angle equal to 114.5°. The difference curve shown in the same figure was obtained using the experimental radial distribution curve (shown in Figure 8) calculated with data in the interval $0 \leq s \leq 2.75$ from the theoretical intensity curve corresponding to this free-rotation model.

Despite the improved agreement between the experimental and theoretical radial distribution curves, the free-rotation model of N_2O_5 is quite unrealistic, for it includes planar and near planar conformations which place oxygen atoms from different nitro groups much too close: this distance is 2.2 Å for a central angle of 116.3°, for example, whereas the O. . . O van der Waals distance is about 2.8 Å (Pauling). A simple variant of the free-rotation model obtained by rejecting all conformations having inter-nitro group O. . . O distances less than 2.5 Å was therefore tested. The results were disappointing: the fits to the experimental radial distribution curve were poorer than those given by the free-rotation model. Curve FR' of Figure 9 shows

this for ∠ NON 114.5°.

Tests of more sophisticated restricted-rotation models were carried out by weighting the individual conformation according to $w = w_u \cdot w_v$, where w_u and w_v were of the form $w_u = a + b \cdot \cos(2u) + c \cdot \cos(4u) + d \cdot \cos(6u)$ with u and v the torsional angles of the two NO_2 groups, and forming the theoretical radial distribution curves for the models as described above. Coefficients a, b, c, d for the several weighting functions used are given in Table 23. Two radial distribution curves were usually calculated from these weighting functions, with the second calculation involving the rejection of conformation with inter-nitro group O...O distances less than 2.5 Å. (The weighting functions for these latter calculations will be hereafter designated as 1A', 3C', etc., after the designation given in Table 23 of the corresponding weighting function involving all conformations.) The calculations were initially carried out with ∠ NON 116.3°. Because several features in the difference curves obtained by subtracting the theoretical radial distribution curves from the experimental curve were found to be independent of internal motion, many of the calculations were repeated for central angles of 109.3°, 112.8°, 114.5°, and 123.3°. The difference curves were best for 114.5°, and from a study of the changes it was concluded that roughly equally good fits would be obtained over the range 112°-116° for ∠ NON. Some of the curves resulting from

these calculations of restricted-rotation models are shown in Figure 9 for an NON angle of 114.5°. (All difference curves shown in Figure 9 were calculated from the experimental radial distribution curve shown in Figure 8.)

An examination of the difference curves in Figure 9 is revealing. In addition to the free-rotation model already mentioned, there are many models representing restricted rotation which provide good fits to the experimental radial distribution curve. Of these fits, several appear to be somewhat better than those from free-rotation models. For the models from which these better fitting curves were calculated, conformations with nitro-group torsional angles near 45° and 135° are found to have somewhat higher weights relative to those conformations with torsional angles near 90° and relative to those with torsional angles near 0° and 180° (or inter-nitro group O...O distances less than 2.5 Å). Weighting functions such as 1B, 1C, and 4D of Table 23 give too much weight to conformations with torsional angles near 0° and 180°; weighting functions such as FR', 4A', and most of the series 3 functions give too much weight to conformations with torsional angles near 90°. It is evident from the number of very good fits shown in Figure 9 that the experimental radial distribution curve for N_2O_5 does not contain sufficient information for r values greater than 2.5 Å to allow the determination of the form of the hindering potential.

The calculations just described included contributions from conformations having inter-nitro group O...O distances greater than 2.5 Å. Because this lower limit is rather smaller than the sum of the van der Waals radii, it seemed important to investigate the effect of increasing this limiting value. Accordingly, theoretical radial distribution curves were calculated for models having NON angles of 112.8° and 114.5° using weighting function 1C of Table 23, and adapting 2.6 Å, 2.7 Å, and 2.8 Å for minimum-allowed inter-nitro group O...O distances. Comparison of the resulting curves, shown in Figure 10 for a central angle of 114.5°, with curve 1C' of Figure 9 and the corresponding curve for ∠ NON 112.8°, indicated that the 2.6 Å limit provides the best fit for weighting function 1C. However, this fit is not better than that obtained by using the 2.5 Å limit with other functions.

A step weight function based on values of $r_{O...O}$ between nitro groups was recognized to be somewhat artificial. A more realistic weighting scheme might be $w_{R6} = (r_{O...O} - r_{min})^6$ for $r_{O...O} \leq 1 + r_{min}$, otherwise $w_{R6} = 1$, where r_{min} is a selected constant. This weighting function may be considered to be expressive of a "soft" O...O interaction. Weights for $r_{min} = 1.8$ Å and $r_{min} = 1.7$ Å were calculated for the shortest inter-nitro group O...O distance of each of the unique N_2O_5 conformations having a central angle NON of 114.5°. (The value 1.8 was chosen since it gave a value of $w_{R6} = 1.0$ for $r_{O...O} \leq 2.8$ Å, which is the sum of the van der Waals radii for two oxygen atoms.) The theoretical radial distribution curves

corresponding to individual conformations were then given a weight $w = w_{R6} \cdot w_{1C'}$, where w_{1C} is the weight from function 1C, and the curves were summed and normalized as before. The results of the calculation for $r_{min} = 1.8$ Å are shown in Figure 10, and are thought to be slightly better than those for weighting function 1C'. However, the results are not better than either those obtained with the 2.6 Å limit or some of the results shown in Figure 9 which were based on other weighting schemes for conformations having nitro group torsional angles near 0^{o}, such as those for weighting functions 2A and 2B. The calculation for $r_{min} = 1.7$ Å gave slightly poorer results.

Additional calculations of the type just described seemed to yield no information of importance, and accordingly, further work on the torsional problem was abandoned and attention turned to refinement of the short-range structure of the molecule.

To get the best $O\text{-}NO_2$ group parameters, further least-squares refinements were carried out on a trial structure having an NON angle of 116.3^{o}, nitro group torsion angles of 30.12^{o} and 130.34^{o}, respectively, and values of the remaining parameters as given in Table 22. Using a unitary weight matrix and the composite intensity curve of Figure 7, and allowing all parameters except $\ell_{N...N'}$ $\ell_{O...O'}$ and $\ell_{N...O}$ to vary, two cycles of refinement led to the results shown in Table 24. All non- $O\text{-}NO_2$ group parameters were then fixed at their final values, and a series of additional refinements

involving only the O-NO_2 group parameters was carried out. Initially, all O-NO_2 group parameters were allowed to refine. Then, because of the high correlation among the parameters $\ell_{O_1 \ldots O_2}$, $\ell_{O_2 \ldots O_5}$, and $\angle$ O=N=O, the values of which are involved in the shape and position of the single experimental radial distribution curve peak of 2.2 Å, two additional refinements were carried out, holding first $\angle$ O=N=O and then $\ell_{O_1 \ldots O_2}$ fixed at values near to the final values found for N_2O_4 ($\angle$ O=N=O = 135.3°, $\ell_{O \ldots O}$ = 0.0485 Å). The results of these refinements are given in Table 24, and the theoretical radial distribution and difference curves in the region $r \leq 2.5$ Å are shown in Figure 11. (The experimental curve shown in Figure 11 was calculated using theoretical data in the interval $0 \leq s \leq 2.75$ corresponding to refinement A. Each difference curve shown in Figure 11 was calculated from the experimental curve resulting from use of theoretical data corresponding to that refinement.) From comparison of the difference curves and the values of the agreement factor R, it was concluded that refinement A gave the best O-NO_2 group parameter values. The correlation matrix for refinement A is given in Table 25. The final values for the O-NO_2 parameters, and the associated error limits calculated from equations (3), are given in Table 26.

The refinements of the O-NO_2 parameter values were carried out assuming that the C_2 axis of each nitro group coincided with the corresponding N-O bond. Two deviations from this assumption are

possible. First, the C_2 axis of the nitro group could be out of the plane of the central NON group, i.e., the O-NO_2 group could be non-planar. This would result in a shorter $O_2 \ldots O_5$ distance for the same value of O=N=O angle. The good fit between the experimental and theoretical radical distribution curves assuming planar O-NO_2 groups preclude significant deviation from planarity. Second, the C_2 axis of the nitro group could be in the plane of the second NON group yet not coincide with the N-O bond, i.e., the O-NO_2 group could be planar but not of C_{2v} symmetry. This would give two different $O_2 \ldots O_5$ distances which have a mean of the same value as the single distance resulting from the assumption of coincidence. A least-squares refinement assuming coincidence would then yield a larger than expected mean amplitude of vibration $\ell_{O_2 \ldots O_5}$, and perhaps (because of correlation) a larger than expected mean amplitude $\ell_{O_1 \ldots O_2}$. However, in the present study both $\ell_{O_1 \ldots O_2}$ and $\ell_{O_2 \ldots O_5}$ have been found to have reasonable values, and, if anything, $\ell_{O_1 \ldots O_2}$ is somewhat small. Thus, it is concluded that the assumption made in the refinements is a reasonable one.

Discussion

The results of the present study are in agreement with what has been previously established about the general structure of N_2O_5, i.e., the configuration O_2N-O-NO_2 and C_{2v} symmetry for the O-NO_2 groups.

There are some important differences (Table 26) in the results of the various electron-diffraction studies, however, which deserve comment.

The present results are in general agreement with the preliminary results given by Hedberg and Hedberg. However, they report a 0.02 Å larger N-O mean amplitude and a 0.02 Å shorter N-O bond length than those found in this study. It is felt that both these discrepancies may well result from NO_2 impurity in the N_2O_5 sample used by them, since the possible presence of this impurity was not taken into account in their preliminary refinements. Further refinement of their data in which the presence of NO_2 is included would quite probably bring their results and the present results into better agreement.

The present results are not in agreement with those of Akishin, et al. Their values for the N=O and N-O bond lengths are, respectively, 0.02 Å longer and 0.04 Å shorter than those found in this study, differences which are outside their own (larger) error limits. The value 95° for ∠ NON reported by them is not allowed by the experimental data of the present study. Also, the present study clearly indicates that no single conformation of N_2O_5 can account for the experimental data, and is in disagreement with the non-planar C_{2v} structure reported for the molecule by Akishin, et al. There is agreement between the two studies in regard to the value for ∠ O=N=O, however.

While the present study fails to elucidate completely the rotation-sensitive geometry of covalent N_2O_5, important information about this aspect of the structure has been obtained. The discovery that a large amount of nitro-group torsional motion attends the free molecule is very important, though in fact the motion is responsible for a larger part of the difficulty in determining the value for the central valence NON angle. (The observance of the nitro-group torsional motion supports Hisatsune, Devlin, and Wada [1962] in their statement that their data suggested that in the gas phase the potential barrier against internal rotation of the nitro groups is low.) It would appear, too, that a free-rotation model for the compound is not the best model, since several restricted-rotation models provide better fits to the experimental radial distribution curve. Because these better models tend to have conformations with nitro group torsional angles near 45° and 135° more heavily weighted, one is tempted to conclude that there are intra-molecular interactions which tend to stabilize the coplanar conformations but which are countered by other interactions, such as van der Waals interactions, which prevent the molecule from assuming planarity. The two types of interactions appear to be approximately balanced, since the best fits to the experimental radial distribution curve result from models which include significant contributions from conformations with nitro group torsional angles near both 0° and 90°. The form of the latter interactions is not well determined,

since several variations of weighting for twist angles near 0^{o} (or for distances corresponding to angles near 0^{o}) seem to give good fits. This failure to determine the form of the forces governing the nitro-group rotational motion arises from the fact that differences between the theoretical radial distribution curves corresponding to many of the different rotational models are smaller than the errors in the experimental radial distribution curve. Thus, the experiment itself is incapable of providing enough information to differentiate between various models.

Several aspects of the $O\text{-}NO_2$ group structure are of interest. First, the nitro group geometry is, as it was in N_2O_4, very similar to the geometry of free NO_2 radical (Tables 10, 11, and 26). For the three cases of N_2O_5, N_2O_4, and NO_2, the O=N=O angle values are included in a range of only 2.08^{o}, and the N=O bond lengths in a range of only 0.014 Å. If the difference in temperatures at which the three studies were carried out were to be taken into account, the deviation in the values of the N=O bond length might be even smaller. Also of interest is the somewhat large mean amplitude associated with the N-O bond. (The value 0.0669 Å may be compared to the N-F amplitude found in N_2F_4 of about 0.045 Å [Cardillo and Bauer; Gilbert]). This large amplitude is reasonable when it is considered that the thermal decomposition of N_2O_5 involves the breaking of an N-O bond to form NO_2 and NO_3.

Table 1. . Experimental data for electron-diffraction photographs used in the structure determination of gaseous N_2O_4.

Plate Identification	Plate Size (in)	Accelerating Voltage (volts)	Electron Wavelength[a] (Å)	Beam Current[b] (μa)	Exposure Time (sec)	Bath Temp. (°C)	Nozzle Temp. (°C)	Run-in Pressure (mm Hg)	Camera Height (cm)	s Range
I-108-6	8x10	43772	0.057401	0.10	30	-39	-24	1.0×10^{-5}	75.075	1.0-11.75
I-100-3	5x7	43943	0.057285	0.06	20	-33	-21	3.0×10^{-5}	75.075	1.0-7.50
I-100-4	5x7	43925	0.057297	0.07	40	-36	-22	3.0×10^{-5}	75.075	1.0-8.0
I-100-6	5x7	43895	0.057318	0.07	15	-32	-20	3.0×10^{-5}	75.075	1.0-8.0
I-80-5	8x10	47240	0.055165	0.09	270	-28	-22	1.6×10^{-5}	28.718	12.0-32.25
I-78-5	8x10	47469	0.055025	0.10	150	-31	-19	2.0×10^{-5}	28.770	9.75-32.25[c]
I-214-44	5x7	44400	0.056977	0.70	180	-37	-21	4.8×10^{-6}	12.359	26.0-47.75
I-214-45	5x7	44383	0.056989	0.70	170	-36	-20	4.2×10^{-6}	12.359	24.0-47.75

[a]The wavelengths were calculated from the accelerating voltage, which was calibrated against gaseous CO_2 using $r_a(C-O) = 1.1642$ Å and $r_a(O \ldots O) = 2.3244$ Å. See Plato, Hartford, and Hedberg (1970) for details.

[b]There is some doubt that the recorded values of the beam strength are correct, but the values are unimportant.

[c]For the final least-squares refinement, only the interval $12.0 \leq s \leq 32.25$ of the data were used.

Table 2. Experimental intensity curve (sI_m) for N_2O_4. Data from long camera distance plate I-108-6.

s \ Δs	.00	.25	.50	.75
1.	19	30	28	12
2.	-2	14	-7	16
3.	-11	-84	-244	-481
4.	-768	-1031	-1171	-1055
5.	-668	31	770	1280
6.	1459	1324	989	751
7.	778	831	912	694
8.	203	-362	-935	-1423
9.	-1609	-1563	-1445	-1273
10.	-998	-679	-248	224
11.	777	1329	1607	1665

Table 3. Experimental intensity curve (sI_m) for N_2O_4. Data from long camera distance plate I-100-3.

s \ Δs	.00	.25	.50	.75
1.	20	29	28	12
2.	-3	-14	-7	9
3.	-24	-103	-255	-478
4.	-746	-1005	-1130	-985
5.	-567	76	760	1234
6.	1437	1276	945	732
7.	650	814	908	

Table 4. Experimental intensity curve (sI_m) for N_2O_4. Data from long camera distance plate I-100-4.

s \ Δs	.00	.25	.50	.75
1.	20	34	29	7
2.	-13	-19	-9	5
3.	-24	-110	-288	-529
4.	-824	-1089	-1205	-1004
5.	-539	143	863	1313
6.	1468	1321	1015	775
7.	720	829	882	743
8.	337			

Table 5. Experimental intensity curve (sI_m) for N_2O_4. Data from long camera distance plate I-100-6.

s \ Δs	.00	.25	.50	.75
1.	20	33	30	12
2.	-4	-17	-8	6
3.	-27	-108	-276	-509
4.	-786	-1028	-1155	-991
5.	-580	63	819	1325
6.	1493	1306	967	723
7.	679	785	865	728
8.	276			

Table 6. Experimental intensity curve (sI_m) for N_2O_4. Data from middle camera distance plate I-80-5.

s \ Δs	.00	.25	.50	.75
12.	1494	1362	1186	908
13.	440	-289	-1099	-1712
14.	-1945	-1809	-1426	-919
15.	-548	-286	-115	-2
16.	179	453	710	931
17.	1201	1356	1469	1550
18.	1453	1062	311	-608
19.	-1524	-2109	-2322	-2108
20.	-1576	-933	-292	103
21.	402	582	736	800
22.	999	1197	1267	1344
23.	1401	1180	806	246
24.	-495	-1305	-1871	-2168
25.	-2018	-1658	-1127	-487
26.	-9	414	692	932
27.	969	1019	1063	1044
28.	867	936	646	488
29.	192	-207	-571	-1121
30.	-1492	-1570	-1549	-1361
31.	-1022	-581	-125	358
32.	652	924		

Table 7. Experimental intensity curve (sI_m) for N_2O_4. Data from middle distance plate I-78-5.[a]

s \ Δs	.00	.25	.50	.75
9.	....	....	....	-1244
10.	-1027	-734	-360	172
11.	750	1177	1469	1520
12.	1453	1322	1183	932
13.	512	-126	-937	-1591
14.	-1956	-1919	-1527	-1019
15.	-585	-273	-73	71
16.	242	508	808	1061
17.	1212	1331	1446	1498
18.	1357	1008	424	-476
19.	-1408	-2126	-2339	-2191
20.	-1701	-1124	-509	-52
21.	309	515	667	787
22.	948	1092	1240	1334
23.	1264	1109	769	265
24.	-391	-999	-1570	-2094
25.	-2126	-1727	-1102	-485
26.	4	412	676	821
27.	865	955	1019	1145
28.	1170	1194	1023	776
29.	443	-6	-619	-1047
30.	-1391	-1585	-1570	-1370
31.	-868	-655	-112	431
32.	600	985		

[a] Data in the interval $12.0 \leq s \leq 32.25$ only was used in the final refinement.

Table 8. Experimental intensity curve (sI_m) for N_2O_4. Data from short camera distance curve I-214-44.

s \ Δs	.00	.25	.50	.75
26.	-358	165	503	819
27.	1018	1129	1190	1257
28.	1236	1094	809	526
29.	194	-225	-664	-981
30.	-1335	-1551	-1513	-1323
31.	-1059	-649	-334	78
32.	372	688	957	1185
33.	1180	1112	1130	886
34.	643	257	-134	-350
35.	-550	-805	-1057	-1223
36.	-1119	-852	-821	-479
37.	-174	148	354	460
38.	761	784	792	749
39.	684	277	174	25
40.	-312	-375	-494	-606
41.	-580	-535	-489	-500
42.	-338	-149	111	394
43.	673	703	736	596
44.	597	361	305	2
45.	-252	-341	-458	-574
46.	-453	-412	-419	-402
47.	-283	-107	-35	58

Table 9. Experimental intensity curve (sI_m) for N_2O_4. Data from short camera distance plate I-214-45.

s \ Δs	.00	.25	.50	.75
24.	-19	-890	-1735	-2181
25.	-2301	-2108	-1636	-798
26.	-167	247	601	883
27.	1068	1230	1226	1127
28.	1178	1099	821	721
29.	344	-40	-463	-657
30.	-1157	-1481	-1508	-1437
31.	-1188	-700	-233	76
32.	471	629	795	965
33.	1026	958	897	847
34.	596	181	-15	-62
35.	-446	-623	-839	-861
36.	-898	-860	-672	-493
37.	-61	252	506	838
38.	1015	868	843	829
39.	389	98	-98	-258
40.	-332	-413	-521	-517
41.	-314	-682	-598	-256
42.	-257	-1	179	397
43.	360	492	619	454
44.	602	506	299	183
45.	38	-251	-556	-556
46.	-440	-502	-516	-394
47.	-182	2	-39	122

Table 10. Gaseous NO_2 parameter values used in least-squares refinements of gaseous N_2O_4.[a]

Parameter	Experimental[b]	Calculated[c]	"Corrected" Experimental[d]
$r_{N-O}(107^oC)$	1.202	....	....
$r_{O...O}(107^oC)$	2.213	....	....
$\angle ONO(107^oC)$	134.02	....	....
ℓ_{N-O} (107°C)	0.0382	0.0389	....
ℓ_{N-O} (0°C)	...	0.0387	0.0380
$\ell_{O....O}$ (107°C)	0.0470	0.0484	....
$\ell_{O....O}$ (0°C)	...	0.0471	0.0457

[a]Distances r_a and root-mean-square amplitudes ℓ_a in angstroms, angles in degrees.

[b]The r_a values were used in all refinements. The ℓ_a values were used in the refinements for which the final N_2O_4 parameters were reported. The values are taken from Blank (1964).

[c]The values were supplied by Sven J. Cyvin, and were used to calculate the "corrected" experimental amplitudes.

[d]The values were obtained by subtracting the differences between the calculated amplitudes for 107°C and 0°C from the experimental amplitudes.

Table 11. Parameter values for N_2O_4.[a]

Parameter[b]	This Work		Smith and Hedberg[c]
	r_a, ℓ_a	2σ	r_a, ℓ_a
% N_2O_4	77.5	4.8	>75 (est.)
% NO_2	22.5	9.4	<25 (est.)
r_{N-N}	1.782	0.0083	1.750
r_{N-O}	1.190	0.0018	1.180
$r_{O_1 \ldots O_2}$	2.201	0.0049	2.170
$r_{O_1 \ldots O_2'}$	3.472	0.0071	3.448
$r_{N \ldots O}$	2.490	0.0065	2.465
$r_{O_1 \ldots O_1'}$	2.685	0.0100	2.678
ℓ_{N-N}	0.0816	0.0178	0.0664
ℓ_{N-O}	0.0381	0.0019	0.0424
$\ell_{O_1 \ldots O_2}$	0.0493	0.0040	0.0469
$\ell_{O_1 \ldots O_2'}$	0.0730	0.0114	0.0707
$\ell_{N \ldots O}$	0.0729	0.0061	0.0707
$\ell_{O_1 \ldots O_1'}$	0.0970	0.0167	0.0848
$\angle$ONO	135.39	0.58	133.7
R[d]	0.137		

[a] Distances r_a and root-mean-square amplitudes ℓ_a in angstroms, angles in degrees. The 2σ values include estimates of both systemic and random error. The r_a and ℓ_a values differ slightly from r_e. See Hedberg and Iwasaki (1962).

[b] See Figure 5 for the molecule.

[c] Smith and Hedberg (1956).

[d] $R = [\Sigma \omega_i \Delta_i^2 / \Sigma \omega_i I_i^2 (\text{obs})]^{\frac{1}{2}}$, where $\Delta_i = I_i(\text{obs}) - I_i(\text{calc})$.

Table 12. Correlation matrix for N_2O_4 parameters[a].

$\%N_2O_4$	$\%NO_2$	ℓ_{N-N}	ℓ_{N-O}	$\ell_{O_1 \ldots O_2}$	$\ell_{O_1 \ldots O_2'}$	ℓ_{N-O}	$\ell_{O_1 \ldots O_1'}$	r_{N-N}	r_{N-O}	$r_{O_1 \ldots O_2}$	$r_{O_1 \ldots O_2'}$	$r_{N \ldots O}$	$r_{O_1 \ldots O_1'}$	$\angle ONO$
1.00	-0.93	0.19	0.32	0.04	0.31	0.53	0.13	-0.19	0.72	0.24	0.25	0.01	0.12	-0.18
	1.00	-0.20	-0.04	0.07	-0.29	-0.49	-0.12	0.19	-0.77	-0.25	-0.28	-0.03	-0.14	0.19
		1.00	0.03	-0.10	0.08	0.06	-0.03	0.03	0.13	0.09	0.07	0.05	0.02	0.01
			1.00	0.20	0.09	0.18	0.06	-0.02	0.04	0.02	-0.01	-0.02	-0.02	0.00
				1.00	0.02	0.03	-0.00	-0.11	-0.03	-0.02	-0.13	-0.14	-0.10	0.00
					1.00	0.14	0.03	-0.04	0.21	0.09	0.06	0.00	0.02	-0.03
						1.00	0.34	-0.09	0.40	0.23	0.07	-0.04	-0.03	-0.00
							1.00	-0.08	0.10	0.13	-0.11	-0.13	-0.14	0.07
								1.00	-0.30	0.40	0.38	0.79	0.17	0.55
									1.00	0.22	0.40	0.03	0.25	-0.35
										1.00	-0.28	-0.04	-0.61	0.84
											1.00	0.86	0.93	-0.50
												1.00	0.73	-0.05
													1.00	-0.72
														1.00

[a]Distances and root-mean-square amplitudes in angstroms, angles in degrees. The matrix is symmetric.

Table 13. Experimental data for electron-diffraction photographs used in the structure determination of gaseous N_2O_5.

Plate Identification	Plate Size (in)	Accelerating Voltage (volts)	Electron Wavelength[a] (Å)	Beam Current (μa)	Exposure Time (sec)	Bath Temp. (°C)	Nozzle Temp. (°C)	Run-in Pressure (mm Hg)	Camera Height (cm)	s range
I-287-6	5x7	43773	0.057401	0.46	20	-9.7	-10	3.0×10^{-6}	74.894	1.0-8.50
I-287-7	5x7	43774	0.057400	0.46	30	-9.7	-12	3.0×10^{-6}	74.894	1.0-8.50
I-287-8	8x10	43777	0.057398	0.46	30	-9.5	-13	3.0×10^{-6}	74.905	1.0-13.25
I-287-9	8x10	43778	0.057397	0.46	40	-9.5	-12	2.9×10^{-6}	74.905	1.0-13.25
I-286-7	8x10	43756	0.057412	0.50	120	-10	-11	4.0×10^{-6}	29.922	8.0-32.25
I-286-3	8x10	43792	0.057388	0.48	150	-11	-10	3.3×10^{-6}	29.922	8.0-32.25
I-291-3	8x10	43835	0.057358	0.38	540	-9	-11	3.0×10^{-6}	11.948	25.0-55.50
I-291-2	8x10	43826	0.057365	0.38	480	-9	-10	3.5×10^{-6}	11.948	25.0-48.50

[a]The wavelengths were calculated from the accelerating voltage, which was calibrated against gaseous CO_2 using $r_a(C-O) = 1.1642$ Å and $r_a(O \ldots O) = 2.3244$ Å. See Plato, Hartford, and Hedberg for details.

Table 14. Experimental intensity curve (sI_m) for N_2O_5. Data from long camera distance plate I-287-6.

s \ Δs	.00	.25	.50	.75
1.	10	17	15	9
2.	-1	-17	-36	-58
3.	-77	-89	-125	-212
4.	-340	-464	-536	-490
5.	-321	-36	313	632
6.	879	971	897	658
7.	373	60	-238	-428
8.	-581	-603	-501	

Table 15. Experimental intensity curve (sI_m) for N_2O_5. Data from long camera distance plate I-287-7.

s \ Δs	.00	.25	.50	.75
1.	15	21	16	8
2.	-4	-23	-47	-64
3.	-78	-96	-142	-252
4.	-405	-558	-641	-599
5.	-408	-64	370	804
6.	1128	1252	1143	858
7.	467	76	-278	-548
8.	-746	-812	-734	

Table 16. Experimental intensity curve (sI_m) for N_2O_5. Data from long camera distance plate I-287-8.

s \ Δs	.00	.25	.50	.75
1.	16	28	22	9
2.	-7	-30	-57	-83
3.	-112	-132	-192	-323
4.	-520	-724	-851	-818
5.	-579	-126	463	1052
6.	1498	1663	1532	1154
7.	608	80	-381	-731
8.	-934	-946	-739	-399
9.	-105	74	-44	-379
10.	-749	-964	-980	-708
11.	-234	423	1034	1478
12.	1628	1514	1200	711
13.	270	-113		

Table 17. Experimental intensity curve (sI_m) for N_2O_5. Data from long camera distance plate I-287-9.

s \ Δs	.00	.25	.50	.75
1.	19	32	29	19
2.	2	-23	-64	-99
3.	-143	-177	-249	-404
4.	-635	-886	-1043	-1034
5.	-777	-262	438	1183
6.	1835	2093	1884	1328
7.	662	-0	-554	-967
8.	-1201	-1192	-952	-509
9.	-112	104	-55	-446
10.	-858	-1170	-1183	-847
11.	-263	579	1335	1919
12.	2075	1933	1450	854
13.	303	-138		

Table 18. Experimental intensity curve (sI_m) for N_2O_5. Data from middle distance plate I-286-7.

s \ Δs	.00	.25	.50	.75
8.	-1033	-992	-730	-389
9.	-101	52	-66	-367
10.	-746	-1036	-1028	-723
11.	-176	617	1306	1819
12.	1942	1773	1299	628
13.	50	-486	-914	-1161
14.	-1200	-996	-724	-510
15.	-532	-680	-892	-975
16.	-763	-311	299	928
17.	1598	2010	2211	2123
18.	1650	844	-79	-916
19.	-1616	-2032	-2189	-1957
20.	-1547	-1062	-551	-198
21.	20	257	423	714
22.	947	1158	1357	1410
23.	1432	1324	790	292
24.	-400	-1044	-1626	-1760
25.	-1729	-1622	-1130	-625
26.	-232	266	584	761
27.	954	1060	869	836
28.	793	655	445	310
29.	84	-77	-625	-911
30.	-1272	-1382	-1305	-1375
31.	-1089	-815	-384	-27
32.	321	525		

Table 19. Experimental intensity curve (sI_m) for N_2O_5. Data from middle distance plate I-286-3.

s \ Δs	.00	.25	.50	.75
8.	-1051	-1049	-840	-429
9.	-67	62	-93	-405
10.	-760	-1076	-1080	-778
11.	-149	647	1367	1826
12.	1929	1754	1300	687
13.	42	-520	-961	-1263
14.	-1269	-1095	-818	-588
15.	-533	-750	-932	-998
16.	-897	-456	204	847
17.	1510	2004	2190	2155
18.	1733	1008	75	-799
19.	-1592	-2031	-2206	-2050
20.	-1637	-1056	-574	-161
21.	89	319	505	801
22.	1020	1177	1346	1452
23.	1441	1345	904	296
24.	-289	-939	-1487	-1775
25.	-1773	-1466	-1051	-532
26.	-32	374	742	920
27.	965	1086	1027	940
28.	833	738	515	392
29.	220	-40	-472	-870
30.	-1075	-1375	-1368	-1373
31.	-1208	-906	-428	93
32.	434	895		

Table 20. Experimental intensity curve (sI_m) for N_2O_5. Data from short camera distance plate I-291-3.

s \ Δs	.00	.25	.50	.75
25.	-1861	-1771	-1346	-725
26.	-198	367	775	1016
27.	1137	1142	1100	1119
28.	1098	1044	974	858
29.	506	111	-358	-832
30.	-1227	-1528	-1588	-1429
31.	-1392	-1041	-375	315
32.	840	968	1189	1413
33.	1482	1291	1138	936
34.	572	435	-236	-707
35.	-906	-1012	-1048	-1149
36.	-1180	-1021	-990	-814
37.	-304	95	486	918
38.	1080	1501	1321	1336
39.	968	513	1	-308
40.	-337	-359	-534	-750
41.	-513	-786	-732	-385
42.	-365	-373	7	372
43.	560	782	1141	1366
44.	1068	759	682	478
45.	-110	-251	-473	-452
46.	-621	-801	-724	-594
47.	-488	-446	-293	-132
48.	39	450	420	555
49.	803	661	598	238
50.	44	-85	-203	-322
51.	-567	-632	-537	-421
52.	-326	-214	-147	54
53.	211	219	466	459
54.	236	365	200	15
55.	250	213	193	

Table 21. Experimental intensity curve (sI_m) for N_2O_5. Data from short camera distance plate I-291-2.

s \ Δs	.00	.25	.50	.75
25.	-2598	-2331	-1676	-828
26.	-115	548	1113	1472
27.	1764	1822	1491	1546
28.	1358	1082	1128	1221
29.	1029	483	-80	-667
30.	-1357	-1974	-2004	-2050
31.	-1410	-1029	-495	328
32.	906	1413	1687	1819
33.	1808	1553	1230	966
34.	445	194	184	-99
35.	-474	-832	-1102	-1262
36.	-1364	-1409	-1357	-1191
37.	-700	-16	465	626
38.	1124	1663	1280	1116
39.	1128	478	-255	-511
40.	-476	-814	-738	-1002
41.	-999	-969	-666	-474
42.	-436	-83	92	325
43.	774	1173	1345	1249
44.	1096	907	778	400
45.	10	43	-260	-249
46.	-557	-880	-1288	-1010
47.	-587	-479	-450	-64
48.	108	-101	625	

Table 22. Parameter values assumed in calculating theoretical radial distribution curves for N_2O_5.[a]

Parameter[b]	r	ℓ
N_1-O_5	1.500	0.0667
N_1-O_1	1.188	0.0348
$O_1 \ldots O_2$	2.181	0.0419
$O_2 \ldots O_5$	2.252	0.0715
$\angle O_1N_1O_2$	133.39	
$\angle$NON	109.3-123.3	
$\angle u$[c]	0°-90°	
$\angle v$[c]	0°-165°	
N...N	2.447-2.640	0.0920
N...O		0.1000
O...O (other than above)		0.1400

[a]Distances r_a and root-mean-square amplitudes ℓ_a in angstroms, angles in degrees.

[b]The molecule is $O_1O_2N_1$-O_5-$N_2O_3O_4$. See Figure 6.

[c]Nitro group torsional angles. 0° corresponds to a nitro group being coplanar with the central NON group, and positive angle increase is in the clockwise direction. The range of values indicated give all unique conformations for a given $\angle$NON.

Table 23. Coefficients for the weighting functions $w_u = a+b\cdot\cos(2u)+c\cdot\cos(4u)+d\cdot\cos(6u)$ used in calculating theoretical radial distribution curves for restricted-rotation models of N_2O_5.[a]

Function	a	b	c	d
1A	0.750	0.250	0	0
1B	0.625	0.375	0	0
1C	0.500	0.500	0	0
2A	0.750	0	-0.250	0
2B	0.625	0	-0.375	0
2C	0.500	0	-0.500	0
3A	0.750	0	0	-0.250
3B	0.625	0	0	-0.375
3C	0.500	0	0	-0.500
4A	0.625	0.250	0	-0.250
4B	0.700	0.300	0	-0.150
4C	0.625	0.375	0	-0.188
4D	0.500	0.500	0	-0.250
4E	0.625	0.450	0	-0.150
4F	0.563	0.525	0	-0.175

[a] u is the nitro group torsional angle, and is defined such that u = 0° corresponds to the nitro group being coplanar with the central NON group, and such that the direction of positive angle increase is clockwise rotation.

Table 24. Results of least-squares refinements of O-NO_2 parameter values in N_2O_5[a].

Parameter[b]	2	A		B		C	
	r_a, ℓ_a	r_a, ℓ_a	σ_{LS}	r_a, ℓ_a	σ_{LS}	r_a, ℓ_a	σ_{LS}
$r(N_1-O_5)$	1.499	1.499	0.0021	1.501	0.0023	1.498	0.0022
$r(N_1-O_1)$	1.188	1.188	0.0003	1.187	0.0004	1.187	0.0004
$r(O_1 \ldots O_2)$	2.181	2.181	0.0023	(2.196)		2.186	0.0035
$r(O_1 \ldots O_5)$	2.251	2.251	0.0020	(2.240)		2.246	0.0024
$\ell(N_1-O_5)$	0.0669	0.0669	0.0021	0.0671	0.0022	0.0674	0.0021
$\ell(N_1-O_1)$	0.0349	0.0350	0.0004	0.0351	0.0004	0.0352	0.0004
$\ell(O_1 \ldots O_2)$	0.0421	0.0421	0.0015	0.0460	0.0016	(0.0485)	
$\ell(O_1 \ldots O_5)$	0.0710	0.0710	0.0025	0.0831	0.0024	0.0758	0.0030
$\angle O_1N_1O_2$	133.31	133.31	0.29	(135.30)		133.94	0.43
R[c]	0.1144	0.1144		0.1224		0.1186	
$\angle$NON	115.75	(115.75)		(115.75)		(115.75)	
$\angle u$	29.82	(29.82)		(29.82)		(29.82)	
$\angle v$	130.13	(130.13)		(130.13)		(130.13)	

[a]Distances r_a and root-mean-square amplitudes ℓ_a in angstroms, angles in degrees. The standard errors do not include estimates of systematic error. Parenthesized values not refined. Other amplitudes fixed as follows: $\ell(N \ldots N) = 0.092$; $\ell(N \ldots O) = 0.100$; $\ell(O \ldots O) = 0.140$

[b]The molecule is $O_1O_2N_1-O_5-N_2O_3O_4$. See Figure 6.

[c]$R = [\Sigma \omega_i \Delta_i^2 / \Sigma \omega_i I_i^2 (obs)]^{\frac{1}{2}}$, where $\Delta_i = I_i (obs) - I_i (calc)$.

Table 25. Correlation matrix for O-NO_2 refinement A of N_2O_5.[a]

$\ell(N_1-O_5)$	$\ell(N_1-O_1)$	$\ell(O_{1\ldots}O_2)$	$\ell(O_{2\ldots}O_5)$	$r(N_1-O_5)$	$r(N_1-O_1)$	$r(O_{1\ldots}O_2)$	$r(O_{2\ldots}O_5)$	$\angle O_1N_1O_2$
1.00	0.18	0.07	0.06	-0.02	0.03	0.00	-0.00	-0.01
	1.00	0.20	0.19	0.04	0.03	0.03	0.02	0.02
		1.00	0.49	-0.12	-0.03	0.41	-0.49	0.42
			1.00	0.24	0.06	0.77	-0.45	0.74
				1.00	-0.18	0.35	0.51	0.39
					1.00	0.09	0.14	-0.18
						1.00	-0.55	0.96
							1.00	-0.58
								1.00

[a]Distances and root-mean-square amplitudes in angstroms, angles in degrees. Only elements of the matrix for the O-NO_2 group parameters are included. The matrix is symmetric.

Table 26. Parameter values for N_2O_5 [a].

Parameter [b]	This Work [c]				Akishin, et al. [d]	Hedberg and Hedberg [e]	
	r_a	2σ	ℓ_a	2σ	r	r_a	ℓ_a
N_1-O_5	1.499	0.0060	0.0669	0.0064	1.46 ± 0.02	1.48	0.087
N_1-O_1	1.188	0.0015	0.0349	0.0018	1.21 ± 0.01	1.19	0.039
$O_1 \cdots O_2$	2.181	0.0069	0.0421	0.0045		2.18	0.045
$O_1 \cdots O_5$	2.251	0.0061	0.0710	0.0076		2.23	(0.100)
N···N	[2.514]		(0.0920)		[2.15]	2.50	0.075
$\angle O_1N_1O_2$	133.31	0.82			134 ± 9	134	
∠ NON	114	2			95 ± 2	115	

[a] Distances r and root-mean-amplitudes ℓ in angstroms, angles in degrees. The errors include estimates of both systematic and random error. Values in parenthesis assumed. Values in brackets calculated from other parameter values.

[b] The molecule is $O_1O_2N_1$-O_5-$N_2O_3O_4$. See Figure 6.

[c] The values for the O-NO_2 parameters are from refinement A, Table 24.

[d] Akishin, et al. (1962).

[e] Hedberg and Hedberg (1965).

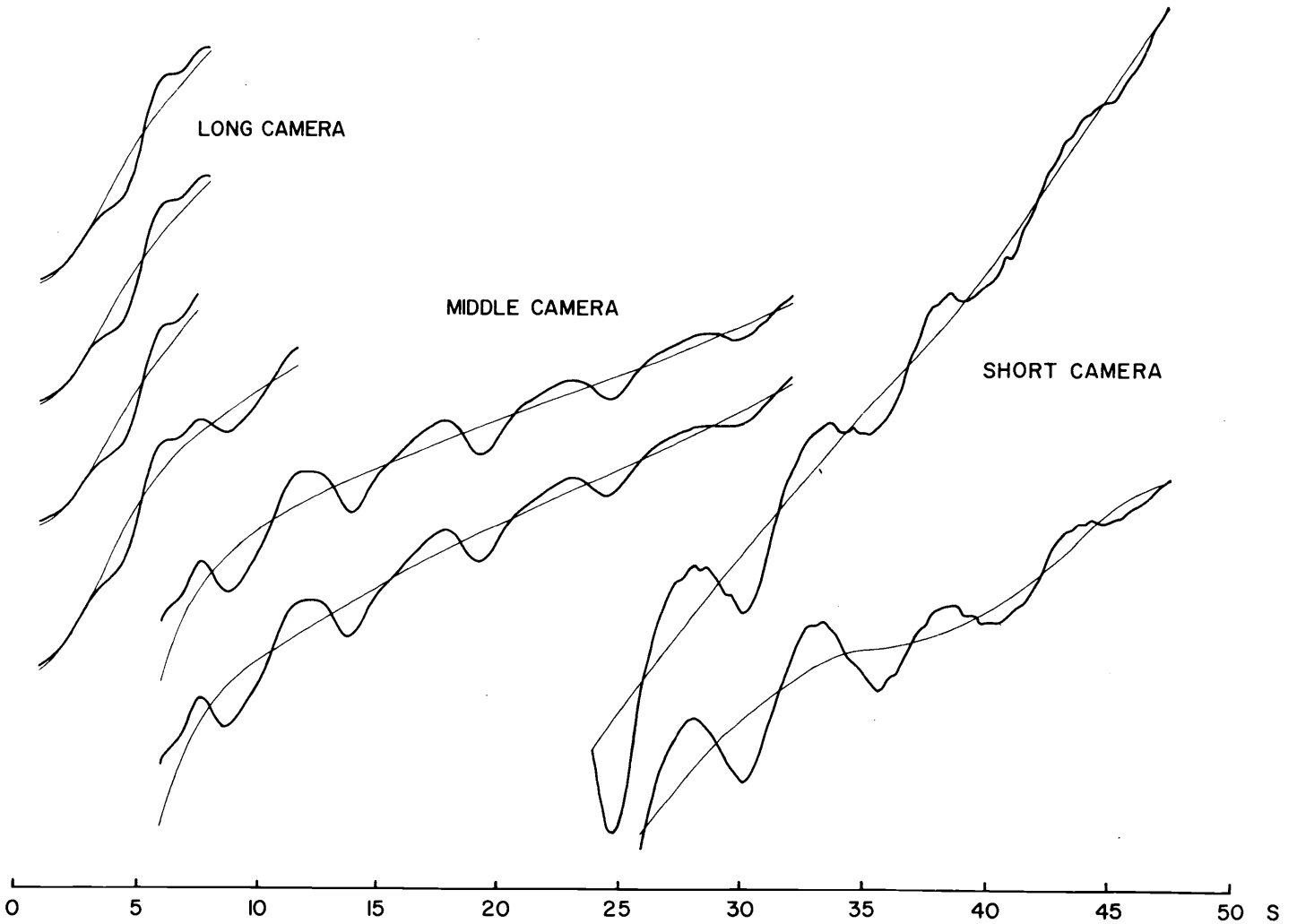

Figure 1. Data-reduction results and final backgrounds for N_2O_4. Middle distance data in the interval $6.0 \leq s \leq 11.75$ was not used in the final refinement.

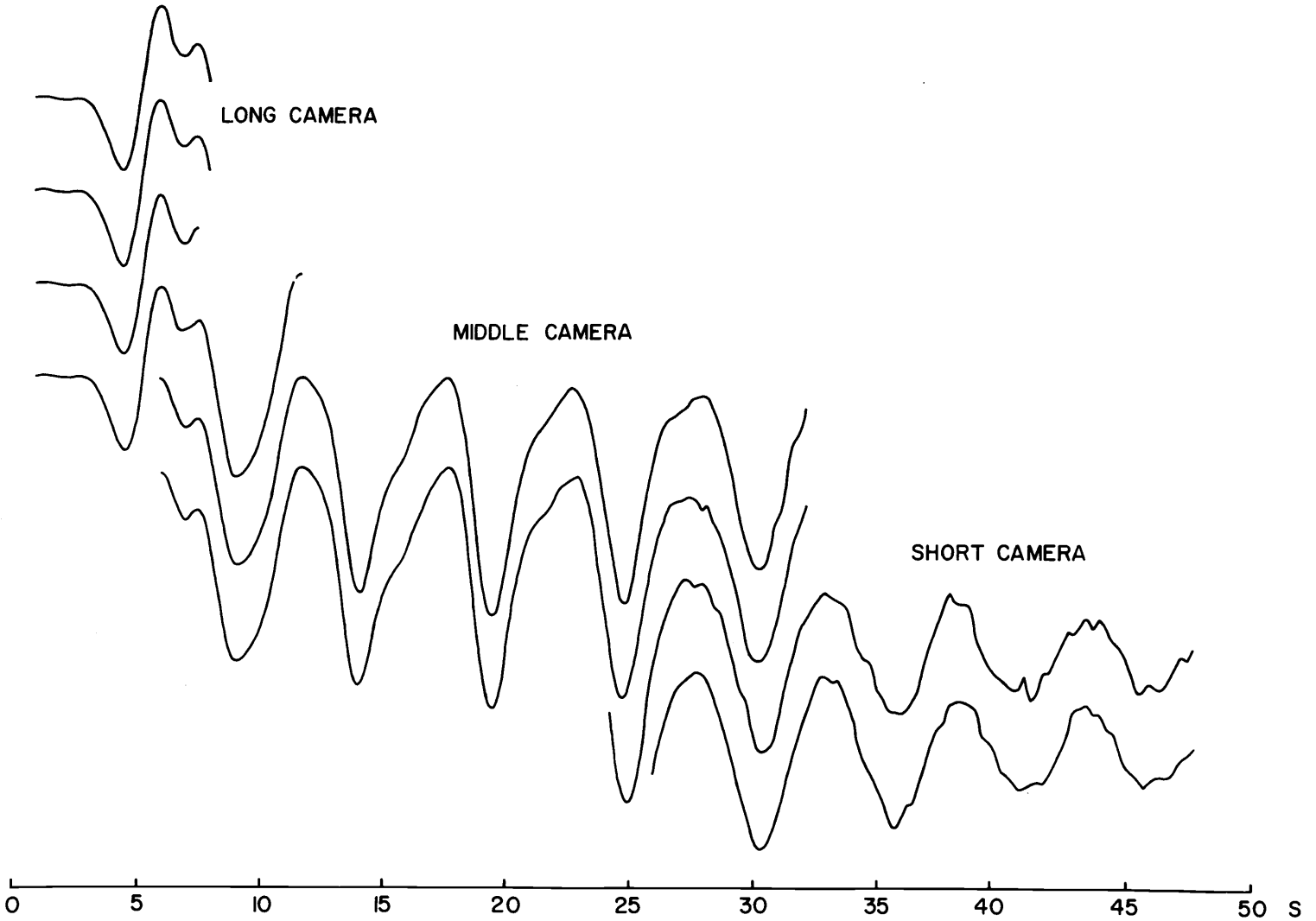

Figure 2. Experimental intensity curves sI_m for N_2O_4. Middle distance data in the interval $6.0 \leq s \leq 11.75$ was not used in the final refinement.

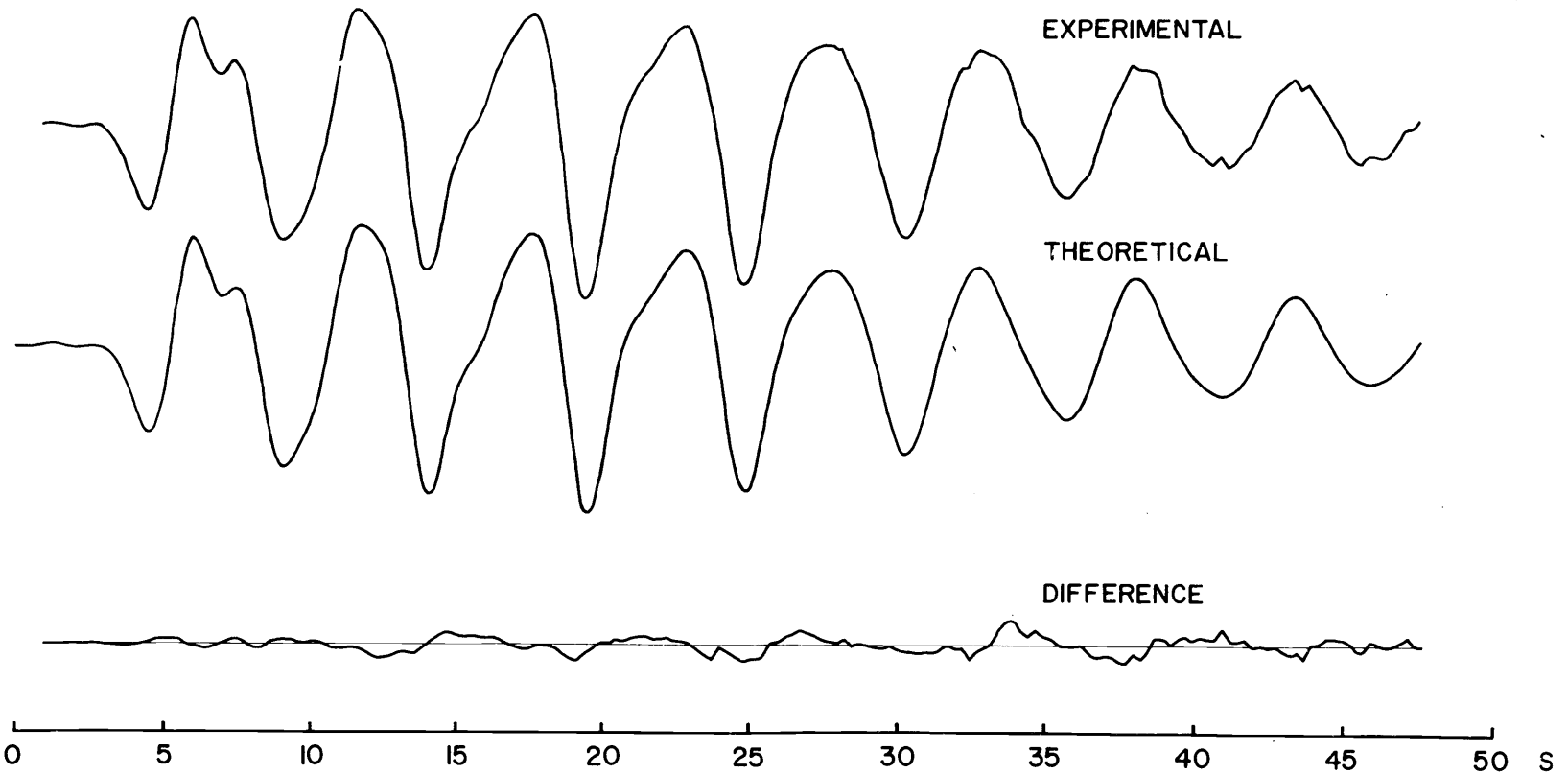

Figure 3. Intensity curves for N_2O_4. The experimental curve is a composite from the curves of Figure 2. The theoretical curve corresponds to the best model obtained from use of all the data of Figure 2.

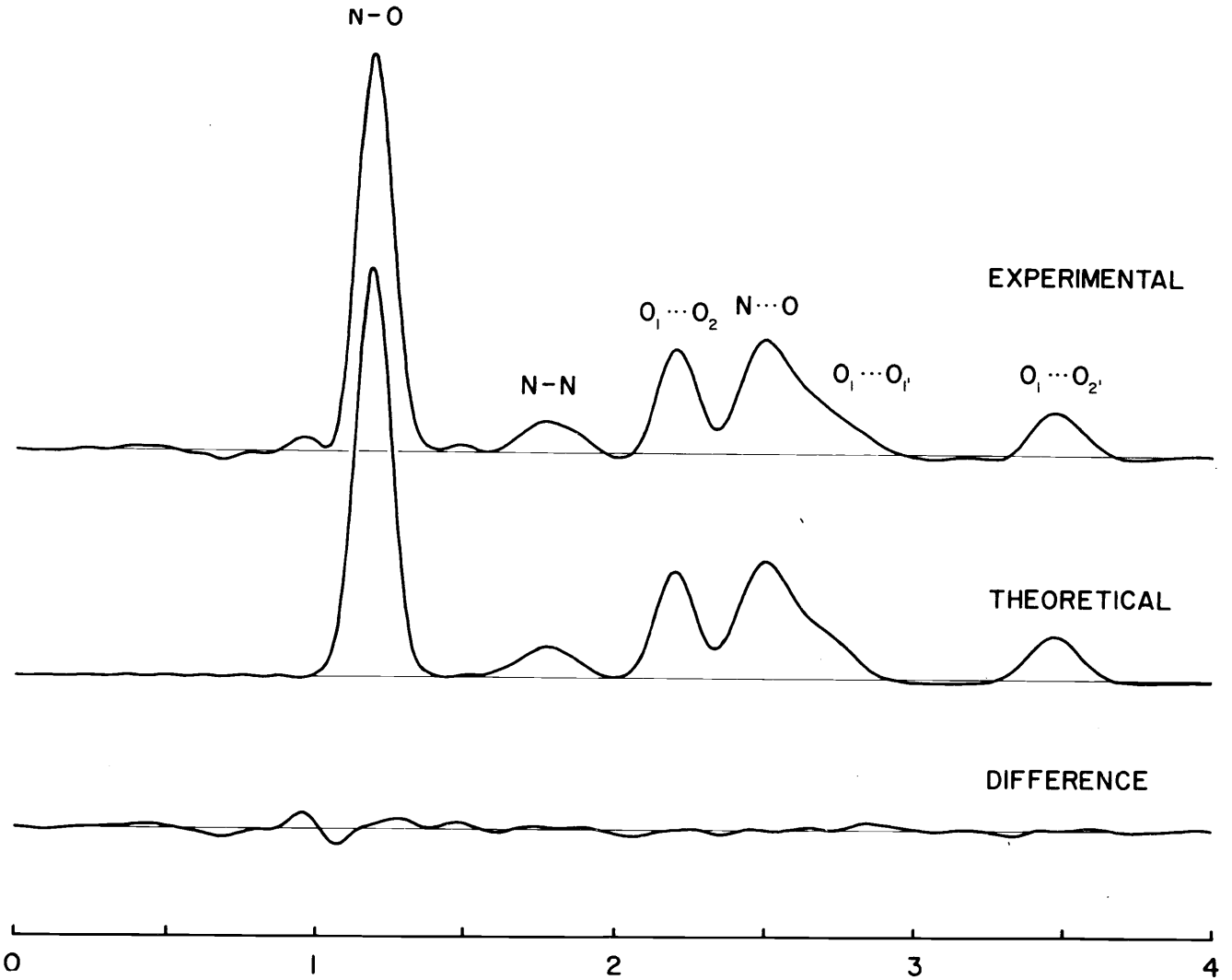

Figure 4. Radial distribution curves for N_2O_4. The curves were calculated from the curves of Figure 3, using theoretical data in the interval $0 \leq s \leq 3.0$ with the composite curve. B = 0.001.

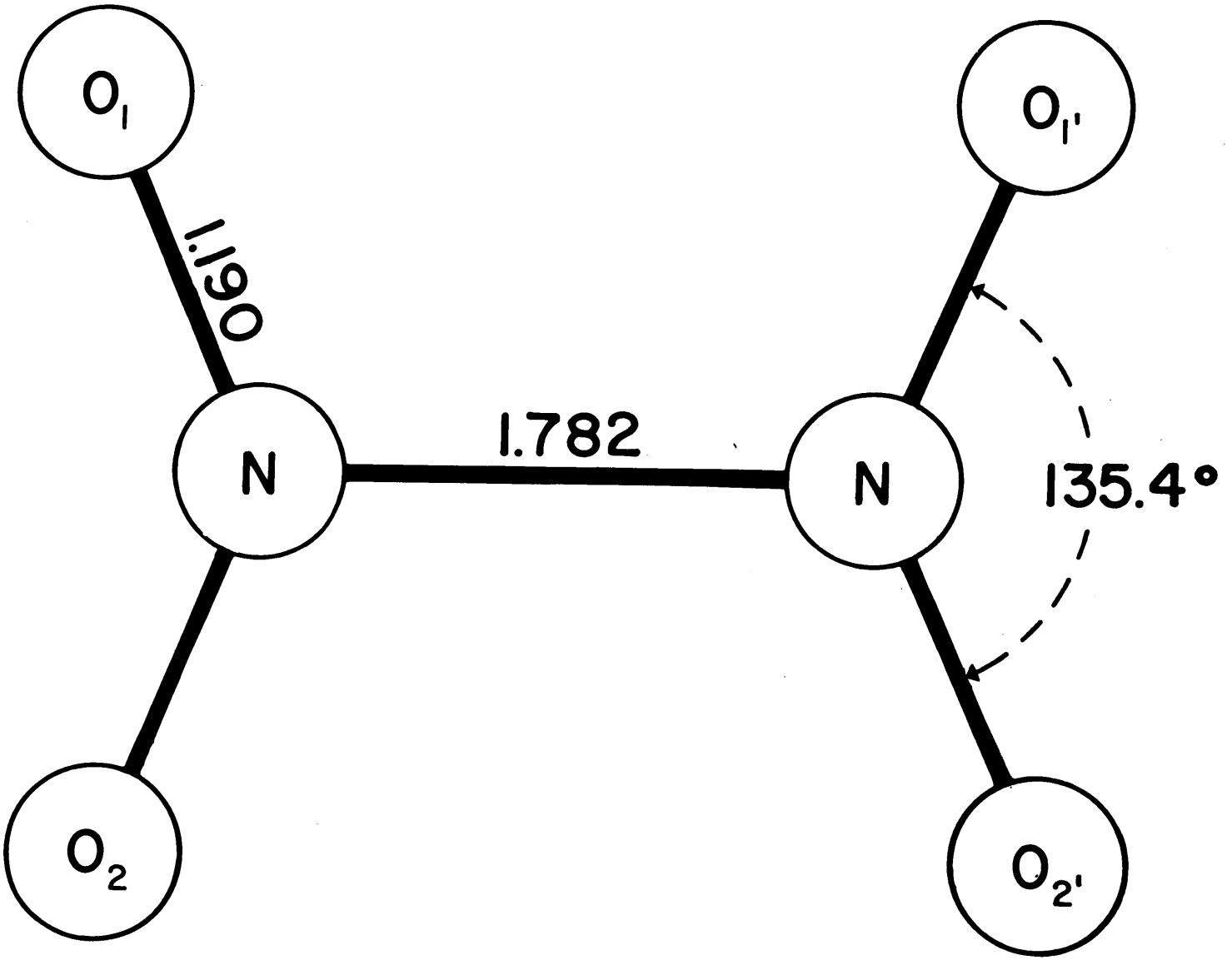

Figure 5. Final model for N_2O_4. Distances in angstroms, angle in degrees.

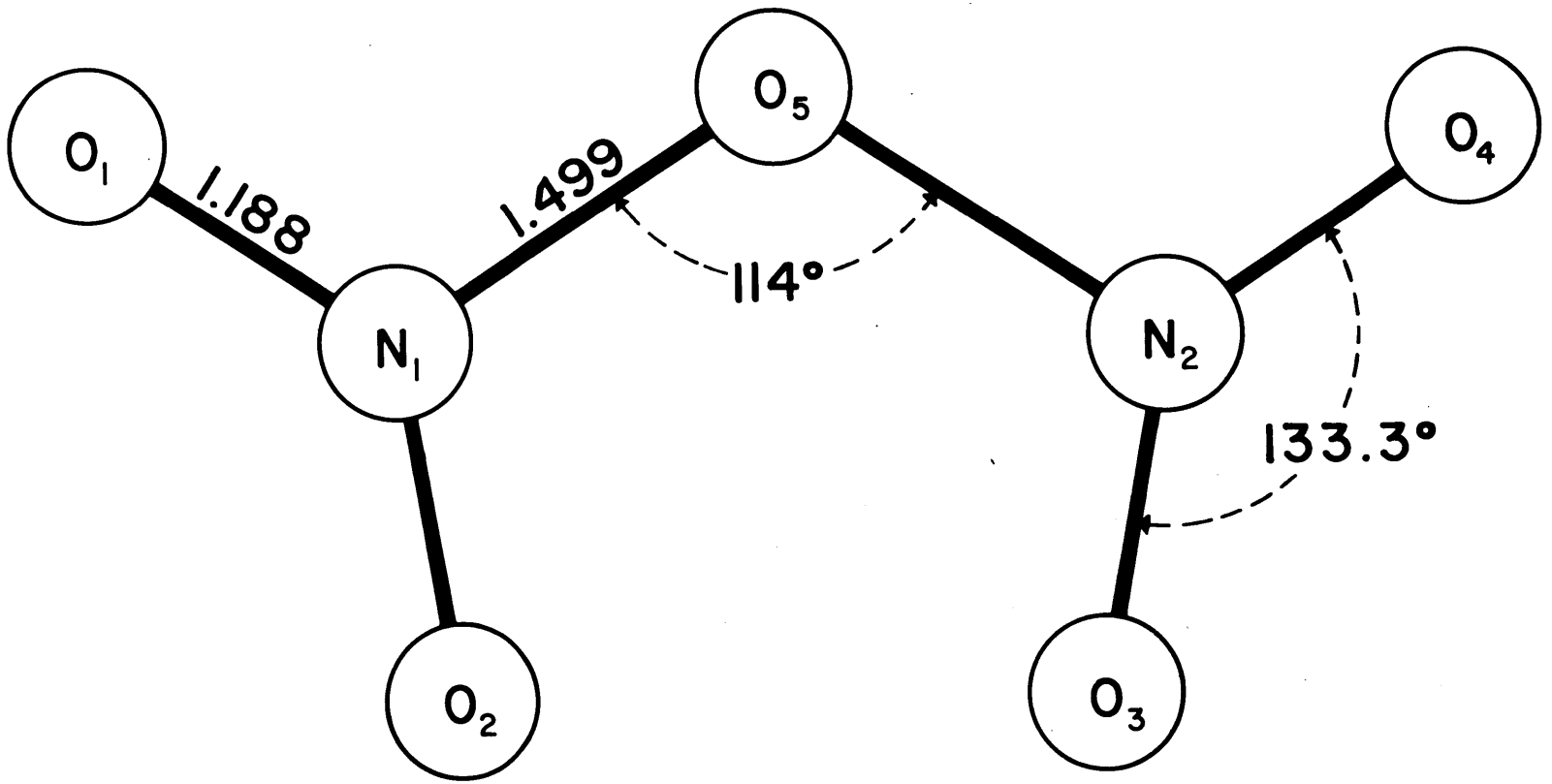

Figure 6. Planar conformation of N_2O_5. Distances in angstroms, angles in degrees.

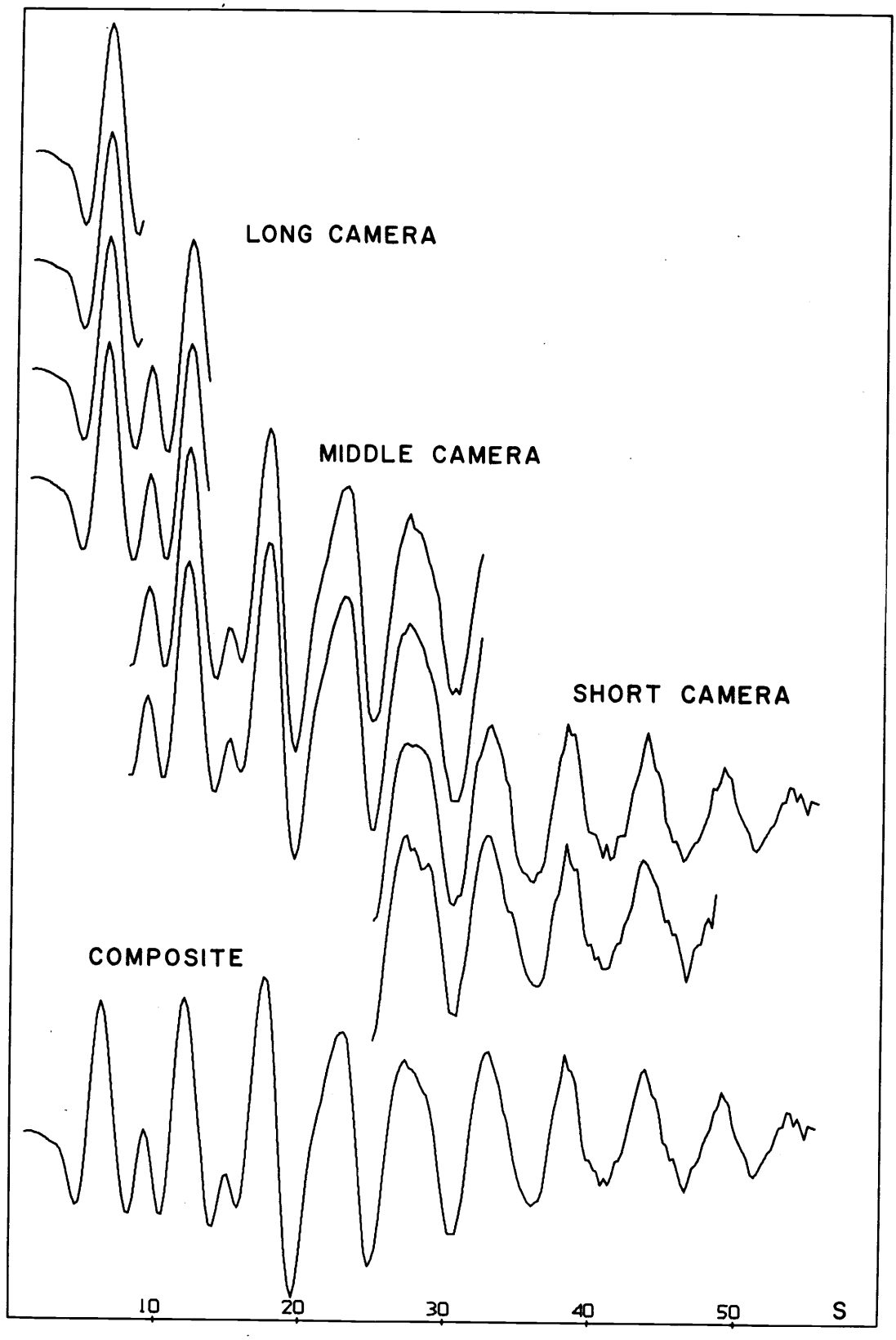

Figure 7. Experimental intensity curves for N_2O_5.

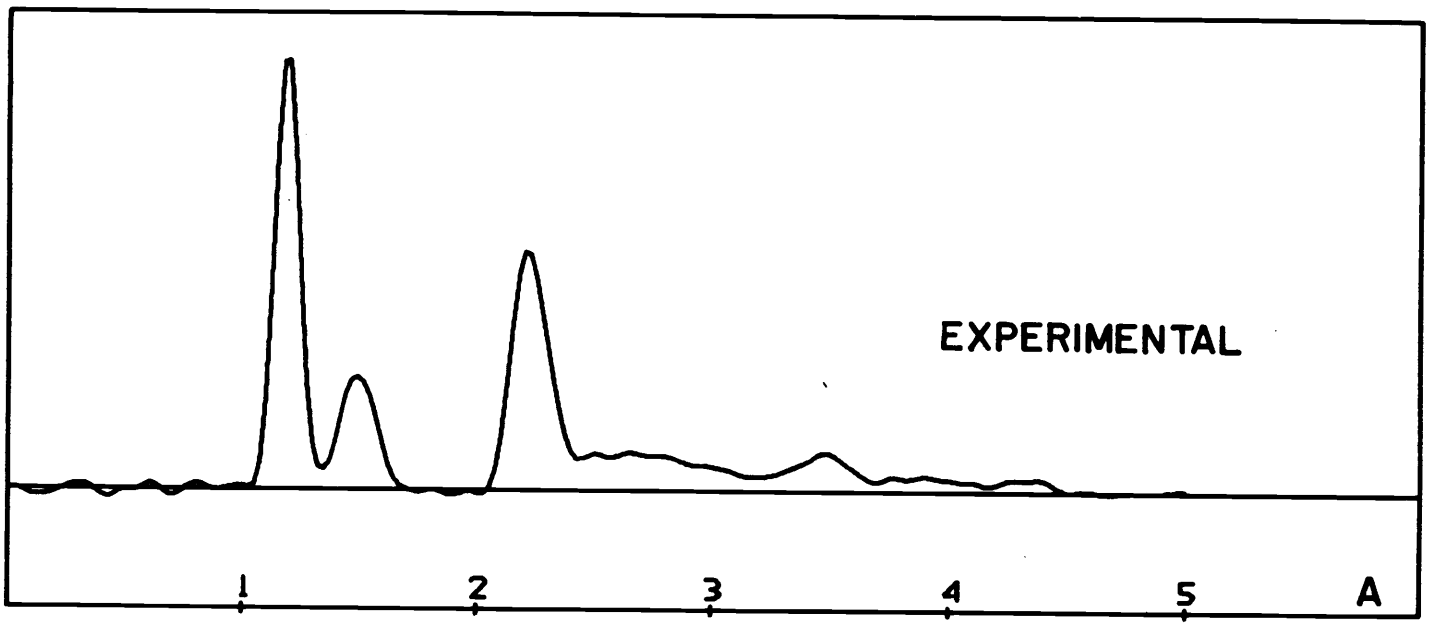

Figure 8. Experimental radial distribution curve for N_2O_5. The curve was calculated from the composite curve of Figure 7 using theoretical data in the interval $0 \leq s \leq 2.75$ corresponding to a free-rotation model for N_2O_5. B = 0.0007.

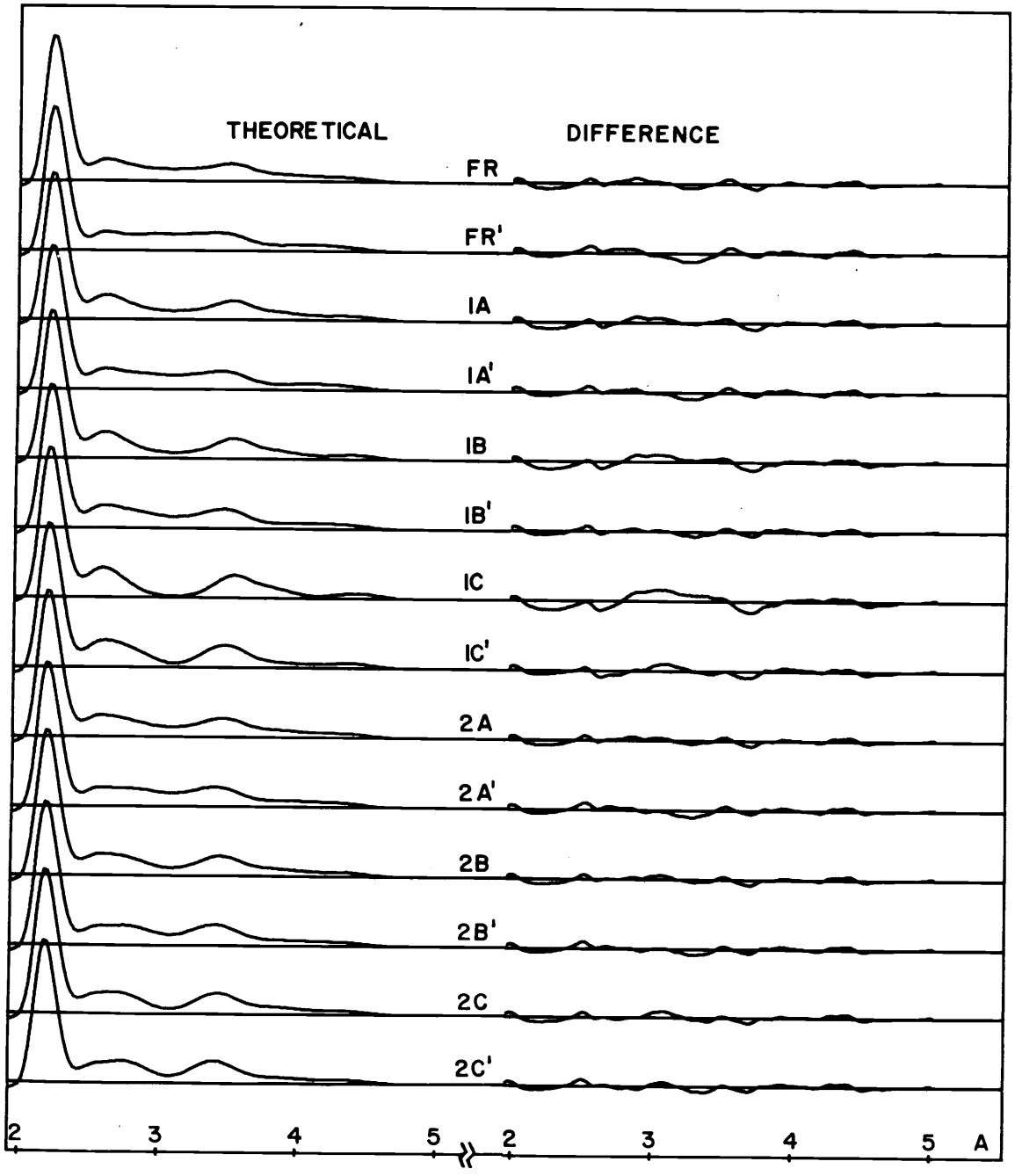

Figure 9. Theoretical radial distribution curves for rotational models of N_2O_5. Curve FR is the free-rotation curve. The other curves were calculated using the weighting functions of Table 23. (See text.) The prime indicates that conformations with inter-nitro group O. . . O distances less than 2.5 Å were assigned zero weight. The difference curves were calculated from the experimental curve of Figure 8.

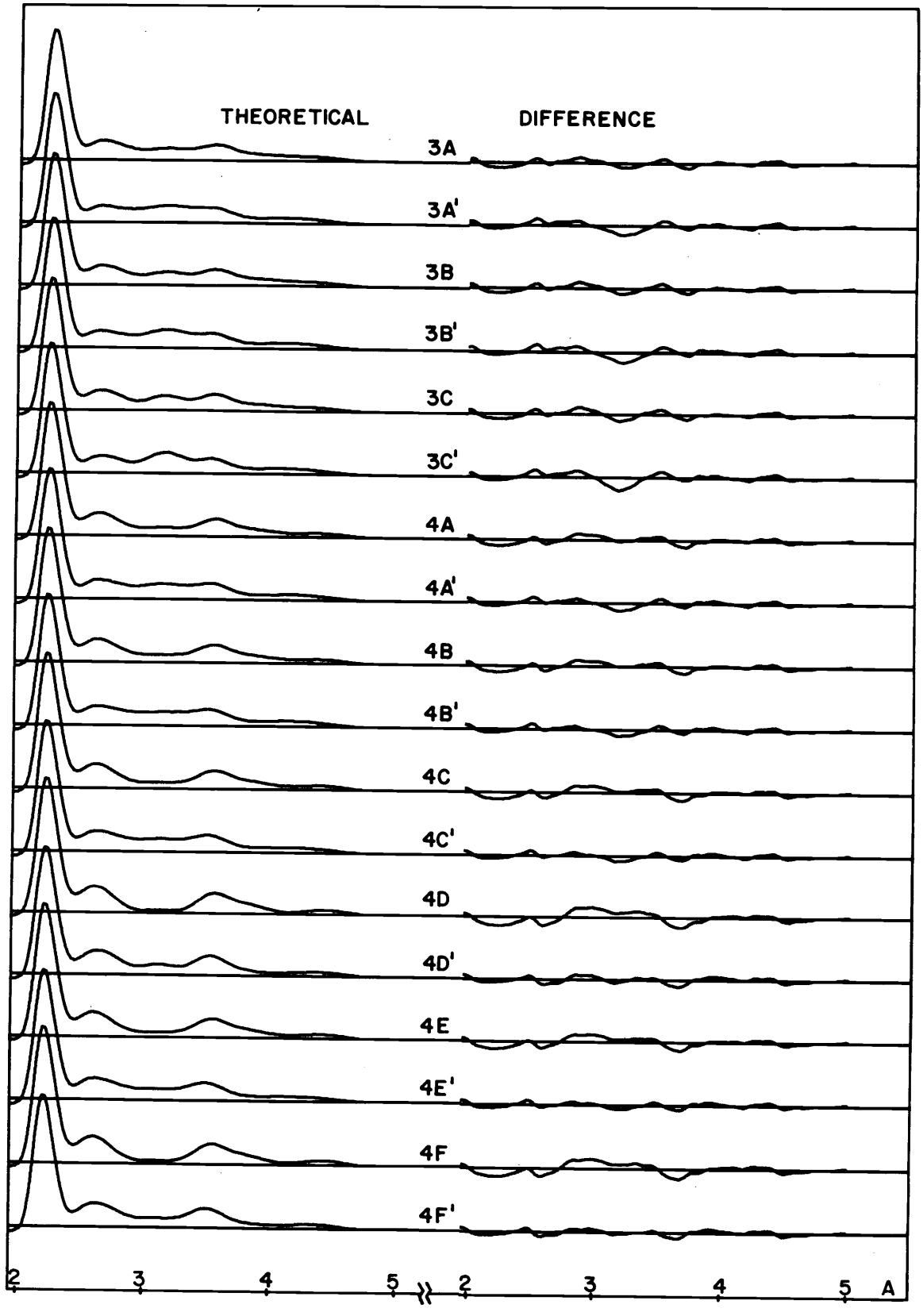

Figure 9. (Cont.)

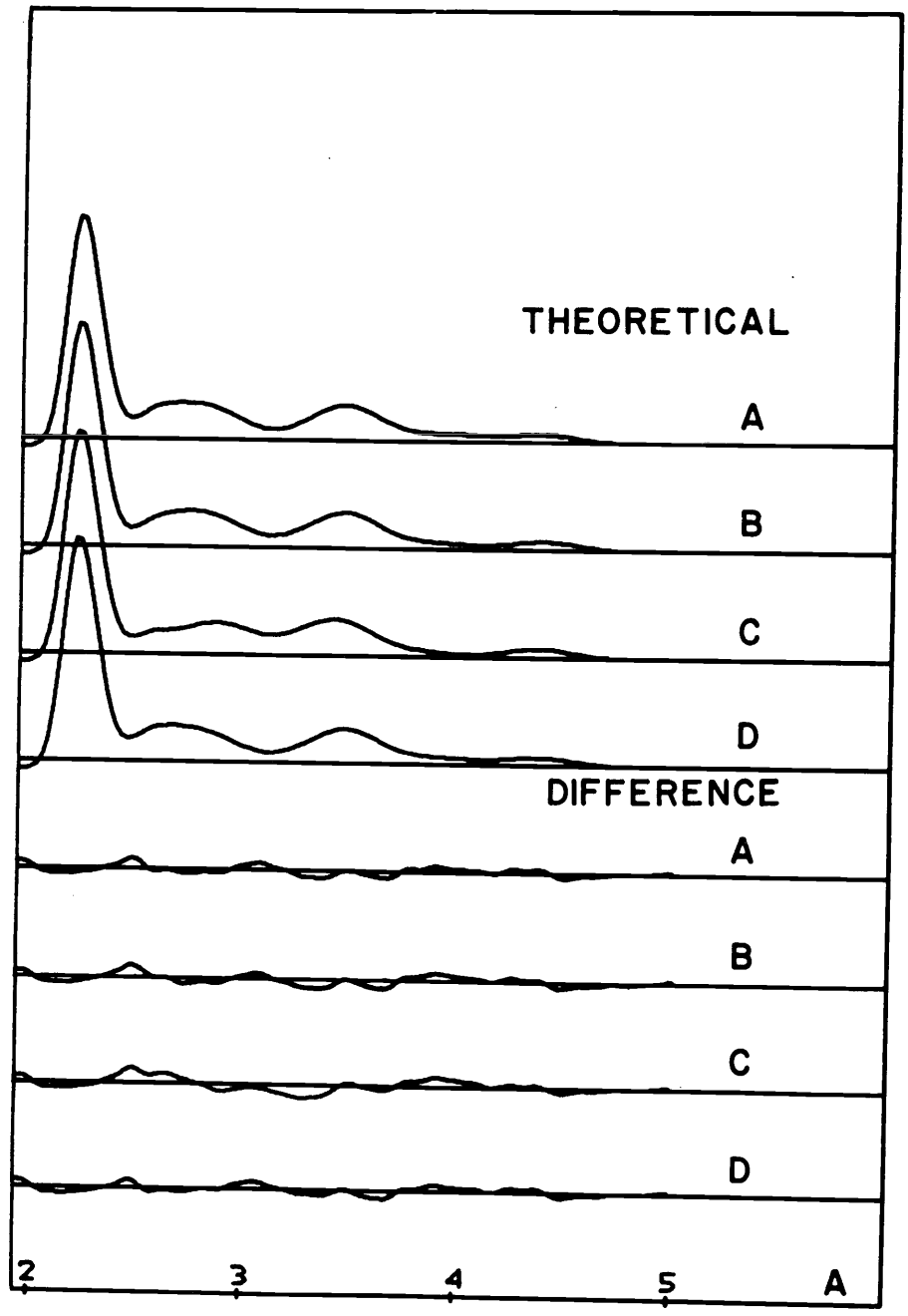

Figure 10. Theoretical radial distribution curves for various models of inter-nitro group oxygen-oxygen interactions in N_2O_5. For all curves, weighting scheme 1C of Table 24 was used. Curves A, B, and C were calculated by rejecting conformations with inter-nitro group O. . . O distances less than 2.6 Å, 2.7 Å, and 2.8 Å, respectively. Curve D was calculated using $w = w_{1C} \cdot w_{R6}$, where w_{R6} is defined in the text. The difference curves were calculated using the experimental curve of Figure 8.

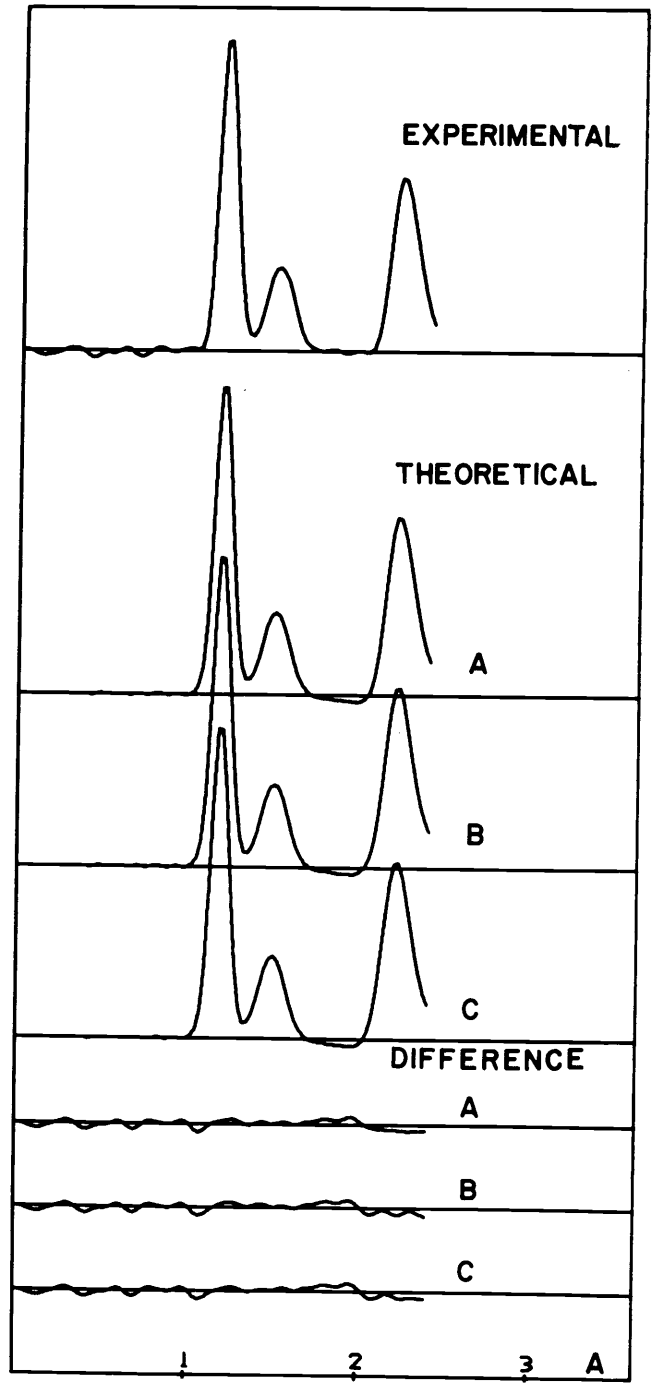

Figure 11. Radial distribution curves for N_2O_5. Curves A, B, and C correspond to the refinements A, B, and C of Table 24, respectively. The experimental curve was calculated using theoretical data in the interval $0 \leq s \leq 2.75$ corresponding to refinement A. Each difference curve was calculated from the experimental curve obtained from use of theoretical data in the interval $0 \leq s \leq 2.75$ corresponding to that refinement.

BIBLIOGRAPHY

P. A. Akishin, et al., J. Phys. Soc. Japan 17 Suppl. B-II, 18 (1962).

D. M. Barnhart, Ph. D. thesis, Oregon State University, Corvallis, 1964.

G. R. Bird, J. Chem. Phys. 25, 1040 (1956).

J. S. Blank, Ph. D. thesis, Oregon State University, Corvallis, 1964.

J. S. Broadley and J. M. Robertson, Nature 164, 914 (1949).

L. O. Brockway, Rev. Mod. Phys. 8, 231 (1936).

R. D. Brown and R. D. Harcourt, Aust. J. Chem. 18, 1885 (1965).

M. J. Cardillo and S. H. Bauer, Inorg. Chem. 8, 2086 (1969).

B. S. Cartwright and J. H. Robertson, Chem. Commun. no. 3, 82 (1966).

J. Chedin, Compt. rend. 203, 772 (1936).

H. L. Cox, Jr., and R. A. Bonham, J. Chem. Phys. 47, 2599 (1967).

R. A. Crawford, Ph. D. thesis, Oregon State University, Corvallis, 1964.

W. G. Fately, H. A. Bent, and B. Crawford, Jr., J. Chem. Phys. 31, 204 (1959).

M. M. Gilbert, Ph. D. thesis, Oregon State University, Corvallis, 1971.

R. Glauber and V. Schomaker, Phys. Rev. 89, 667 (1953).

P. E. Grison, K. Eriks, and J. L. de Vries, Acta Cryst. 3, 290 (1950).

P. Groth, Acta Chem. Scand. 17, 2419 (1963).

G. Gundersen and K. Hedberg, J. Chem. Phys. 51, 2500 (1969).

R. D. Harcourt, Theoret. chim. Acta (Berl.) 6, 131 (1966).

H. Hauptman and J. Karle, Phys. Rev. 77, 491 (1950).

K. Hedberg and L. Hedberg, Structures and Dynamics of Molecules by Electron Diffraction (AD 628060. Avail. CFSTI $3.00 cy, 1965).

K. Hedberg and M. Iwasaki, J. Chem. Phys. 36, 589 (1962).

K. Hedberg and M. Iwasaki, Acta Cryst. 17, 529 (1964).

L. Hedberg, R. R. Ryan, and K. Hedberg, unpublished least-squares program, Department of Chemistry, Oregon State University, Corvallis, 1968.

I. C. Hisatsune, J. Phys. Chem. 65, 2249 (1961).

I. C. Hisatsune, J. P. Devlin, and S. Califano, Spectrochim. Acta 16, 450 (1960).

I. C. Hisatsune, J. P. Devlin, and Y. Wada, J. Chem. Phys. 33, 714 (1960).

I. C. Hisatsune, J. P. Devlin, and Y. Wada, Spectrochim. Acta 18, 1641 (1962).

W. L. Jolly, Synthetic Inorganic Chemistry (Prentice-Hall, Inc., Englewood Cliffs, N. J., 1960).

G. L. Lewis and C. P. Smyth, J. Am. Chem. Soc. 61, 3067 (1939).

Y. Morino, T. Iijima, and Y. Muratu, J. Chem. Soc. Japan 33, 46 (1960).

J. Neisess, Ph. D. thesis, Oregon State University, Corvallis, 1971.

L. Pauling, The Nature of the Chemical Bond (Cornell U. P., Ithaca, N. Y., 1960).

V. Plato, W. D. Hartford, and K. Hedberg, J. Chem. Phys. 53, 3488 (1970).

T. F. Redmond and B. B. Wayland, J. Phys. Chem. 72, 3038 (1968).

R. R. Ryan, Ph. D. thesis, Oregon State University, Corvallis, 1965.

G. Schott and N. Davidson, J. Am. Chem. Soc. 80, 1841 (1958).

D. W. Smith and K. Hedberg, J. Chem. Phys. 25, 1282 (1956).

R. G. Snyder and I. C. Hisatsune, J. Molec. Spectroscopy 1, 130 (1957).

R. Teranishi and J. C. Decius, J. Chem. Phys. 22, 896 (1954).

S. Y. Tyree, Jr. (ed. in chief), Inorganic Synthesis, vol. IX (McGraw-Hill Book Co., N. Y., 1967).

J. Waser and V. Schomaker, Rev. Mod. Phys. 25, 671 (1953).

R. C. Weast (ed. in chief), Handbook of Chemistry and Physics, 48th ed. (The Chemical Rubber Co., Cleveland, Ohio, 1967).

R. N. Wiener and E. R. Nixon, J. Chem. Phys. 26, 906 (1957).